ORIGINAL RESEARCH

CD4$^+$ Regulatory T Lymphocytes Prevent Impaired Cerebral Blood Flow in Angiotensin II-Induced Hypertension

M. Florencia Iulita, PhD;* Sonia Duchemin, PhD;* Diane Vallerand, BSc; Tlili Barhoumi, PhD; Fernando Alvarez, DVM, MSc; Roman Istomine, BSc; Cyril Laurent, PhD; Jessica Youwakim, BSc; Pierre Paradis, PhD; Nathalie Arbour, PhD; Ciriaco A. Piccirillo, PhD; Ernesto L. Schiffrin, MD, PhD; Hélène Girouard, PhD

***Background*—**Immune cells are key regulators of the vascular inflammatory response characteristic of hypertension. In hypertensive rodents, regulatory T lymphocytes (Treg, CD4$^+$CD25$^+$) prevented vascular injury, cardiac damage, and endothelial dysfunction of mesenteric arteries. Whether Treg modulate the cerebrovascular damage induced by hypertension is unknown.

***Methods and Results*—**C57BL/6 mice were perfused with angiotensin II (Ang II; 1000 ng/kg per minute) for 14 days and adoptive transfer of 3×10^5 CD4$^+$CD25$^+$ T cells was performed via 2 intravenous injections. Control mice received a sham surgery and PBS. Treg prevented Ang II-induced neurovascular uncoupling ($P<0.05$) and endothelial impairment ($P<0.05$), evaluated by laser Doppler flowmetry in the somatosensory cortex. The neuroprotective effect of Treg was abolished when they were isolated from mice deficient in interleukin-10. Administration of interleukin-10 (60 ng/d) to hypertensive mice prevented Ang II-induced neurovascular uncoupling ($P<0.05$). Treg adoptive transfer also diminished systemic inflammation induced by Ang II ($P<0.05$), examined with a peripheral blood cytokine array. Mice receiving Ang II + Treg exhibited reduced numbers of Iba-1+ cells in the brain cortex ($P<0.05$) and hippocampus ($P<0.001$) compared with mice infused only with Ang II. Treg prevented the increase in cerebral superoxide radicals. Overall, these effects did not appear to be directly modulated by Treg accumulating in the brain parenchyma, because only a nonsignificant number of Treg were detected in brain. Instead, Treg penetrated peripheral tissues such as the kidney, inguinal lymph nodes, and the spleen.

***Conclusions*—**Treg prevent impaired cerebrovascular responses in Ang II-induced hypertension. The neuroprotective effects of Treg involve the modulation of inflammation in the brain and periphery. **(*J Am Heart Assoc*. 2019;8:e009372. DOI: 10.1161/JAHA.118.009372.)**

Key Words: angiotensin • cerebral blood flow • inflammation • interleukin-10 • lymphocyte

Innate and adaptive immune cells play an important role in the development of hypertension and associated vascular injury.[1] Naïve CD4$^+$ T cells differentiate into 2 main subtypes: conventional effector T helper cells (Th1, Th2, Th9, Th17, Th22, and Tfh), which are involved in cellular inflammation and humoral immunity, and T regulatory lymphocytes (Treg) that express the markers CD4, CD25, and FoxP3, with the latter being the transcription factor that results in commitment of naïve cells to become Treg.[2]

Treg have key roles in maintaining immune homeostasis and act by suppressing immune responses.[3] Multiple mechanisms of Treg-mediated immunosuppression have been

From the Department of Neurosciences (M.F.I., C.L., N.A.), Groupe de recherche sur le système nerveux central (GRSNC) (M.F.I., H.G.), Centre de Recherche du Centre Hospitalier de l'Université de Montréal (CRCHUM) (C.L., N.A.) and Department of Pharmacology and Physiology (S.D., D.V., J.Y., H.G.), Université de Montréal, Montréal, Canada; Lady Davis Institute for Medical Research (T.B., P.P., E.L.S.), Centre of Excellence in Translational Immunology, Research Institute of McGill University Health Centre (F.A., R.I., C.A.P.), Department of Microbiology and Immunology (F.A., R.I., C.A.P.), and Department of Medicine, Sir Mortimer B. Davis-Jewish General Hospital, McGill University, Montréal, Canada (E.L.S.); Centre de recherche de l'Institut universitaire de gériatrie de Montréal, Canada (H.G.).

Dr Tlili Barhoumi is located at King Abdullah International Medical Research Center, King Saud bin Abdulaziz University for Health Sciences, Riyadh, Kingdom of Saudi Arabia.

Accompanying Data S1, Tables S1 through S3 and Figure S1 through S11 are available at https://www.ahajournals.org/doi/suppl/10.1161/JAHA.118.009372

*Dr Iulita and Dr Duchemin contributed equally to this work.

Correspondence to: Hélène Girouard, PhD, Department of Pharmacology and Physiology, Université de Montréal, 2900 Edouard Montpetit, T-439, Montréal (Québec) H3T 1J4 Canada. E-mail: helene.girouard@umontreal.ca

Received April 4, 2018; accepted November 21, 2018.

Clinical Perspective

What Is New?

- This study is the first demonstration that CD4+ regulatory T lymphocytes, at least in part through interleukin-10, prevent impaired cerebral blood flow responses as well as systemic and cerebral inflammation in angiotensin II-induced hypertension.

What Are the Clinical Implications?

- The knowledge that the immune system modulates cerebral blood flow suggests that targeting inflammation or immune cells could protect the brain in conditions where blood flow is impaired, such as hypertension.
- This may also have important clinical implications for cerebral magnetic resonance imaging signaling interpretation.

described. Treg can modulate T effector lymphocytes by secreting anti-inflammatory cytokines such as interleukin-10 (IL-10),[4] or by promoting cell cycle arrest and apoptosis.[5] Treg can also act on antigen-presenting cells by preventing their maturation or limiting their capacity to stimulate the differentiation of effector T cells and thus the release of pro-inflammatory cytokines.[6] In the context of hypertension, it has been shown that Treg (defined as $CD4^+CD25^+$ cells) prevent vascular injury, cardiac damage, and endothelial dysfunction in rodents.[7–10]

Whether $CD4^+CD25^+$ cells can also prevent cerebral blood flow changes induced by hypertension is unknown. The question is pertinent because the brain is one of the principal end-organs that is subject to the deleterious effects of hypertension.[11] With its high metabolic demand, the brain depends on a rigorous control of cerebral blood flow. Thus, it relies on key regulatory mechanisms, such as neurovascular coupling and tightly controlled endothelial dilatory responses to modulate cerebral blood flow. Even small blood flow reductions can have a negative impact on cerebral protein synthesis and neuronal function.[12]

In the case of hypertension, alterations in neurovascular coupling have been seen in humans with untreated high blood pressure, as revealed by reduced cerebral blood flow responses when engaged in a memory task.[13] Experimental rodent models of hypertension induced by angiotensin II (Ang II) recapitulate these deficits, evidenced by impaired neuronal and endothelial cerebral blood flow responses following chronic Ang II infusion.[14,15]

Although the involvement of immune cells in hypertension and peripheral vascular injury is well documented, no studies have yet examined their influence on cerebral blood flow regulation. Likewise, whether $CD4^+CD25^+$ cells could confer neuroprotection to the cerebrovascular injury and brain inflammation induced by Ang II is unclear.

As a first step to answer these questions, we characterized the impact of $CD4^+CD25^+$ regulatory T lymphocytes on cerebral blood flow in vivo, in mice subjected to Ang II-induced hypertension. In view of the potential protective actions of $CD4^+CD25^+$ cells, we also explored systemic immune responses, cerebral gliosis, and superoxide anion production to better understand the cellular targets involved.

Methods

This article adheres to the Transparency and Openness Promotion (TOP) Guidelines. All data, methods, and materials used to conduct the research are available from the corresponding author upon reasonable request.

Animals

The study was approved by the Committee on Ethics of Animal Experiments of Université de Montréal and of the Lady Davis Institute of McGill University, in accordance with the principles outlined by the Canadian Council on Animal Care and by the ARRIVE (Animal Research: Reporting of In Vivo Experiments) guidelines.

Eight- to 10-week-old C57BL/6 male mice (Harlan Laboratories, Canada) were housed individually in a temperature-controlled room with ad libitum access to water and a standard protein rodent diet (Envigo #2018 Teklad global 18% protein rodent diet). C57BL/6 mice with a targeted genetic deletion of IL-10 ($Il10^{-/-}$) and their controls were obtained from a colony bred at the animal facility of the Rosemont-Maisonneuve Hospital Research Center (Montreal, Canada); their original source was The Jackson Laboratory (Maine, USA).

Given that at this age female mice are protected from the deleterious effects of Ang II on cerebrovascular functions,[16] only male mice were used. Following acclimatization, animals were randomly assigned to experimental groups independently of the identity of groups or treatments. Data and animal exclusion criteria are specified for each experiment in Data S1.

Isolation of Treg and Adoptive Transfer

$CD4^+CD25^+$ cells (Treg) were isolated from the spleens of 8- to 10-week-old pathogen-free male C57BL/6 wild-type and $Il10^{-/-}$ mice, using the EasySep Mouse $CD4^+CD25^+$ Treg Cell Isolation kit (Stem Cell Technologies, Canada), as previously described.[17] Determination of cell purity by flow cytometry indicated an enrichment of 89.6% $CD4^+CD25^+$ cells. Mice received 2 intravenous injections (100 µL) of 3×10^5 $CD4^+CD25^+$ (Treg) or $CD4^+CD25^+$ $Il10^{-/-}$ cells (Treg isolated

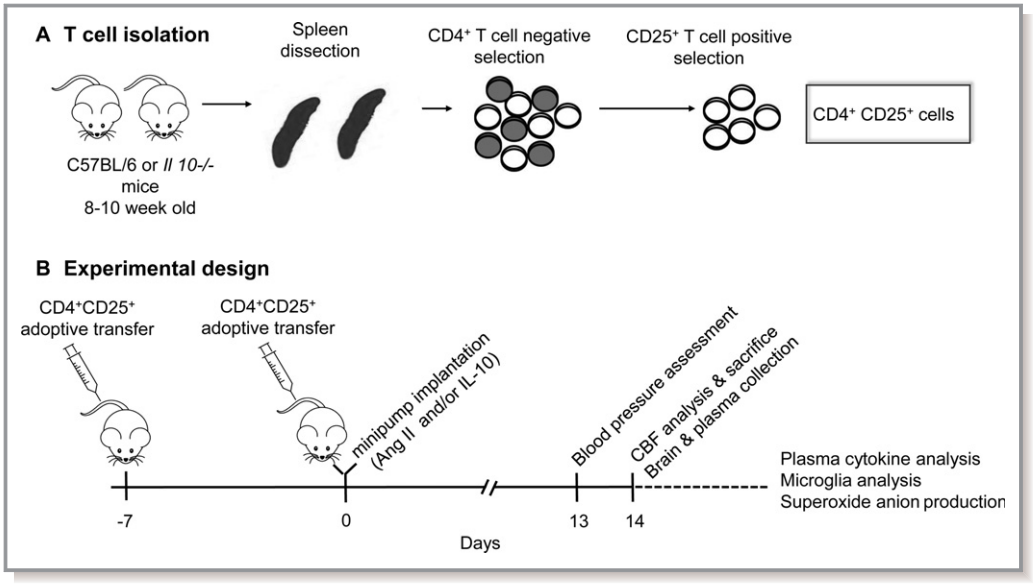

Figure 1. Schematic representation of the T lymphocyte isolation procedure and experimental timeline. **A**, $CD4^+CD25^+$ T lymphocytes were isolated via magnetic bead purification from the spleens of two 8–10-wk-old pathogen-free male C57BL/6 or *Il10*$^{-/-}$ mice. **B**, Mice received 2 intravenous injections of 3×10^5 $CD4^+CD25^+$ cells or $CD4^+CD25^+$ *Il10*$^{-/-}$ cells (isolated from *Il10*$^{-/-}$ mice) or PBS (for the control group). The adoptive transfer injections were done 7 d before and the day of Ang II (1000 ng/kg per min) or IL-10 (60 ng/d for 14 d) minipump implantation. Systolic blood pressure was monitored the day before cerebral blood flow (CBF) analysis and tissue collection. Plasma cytokine analysis, microglia counts, and assessment of superoxide anion production were performed afterwards.

from *Il10*$^{-/-}$ mice) or PBS 7 days before and the day of minipump implantation (Figure 1).

Chronic Angiotensin II and IL-10 Infusion

Osmotic minipumps (model 1002; Alzet, USA) containing human Ang II (Millipore-Sigma, USA) were implanted as detailed in Data S1. Each minipump delivered 1000 ng/kg per minute Ang II for 14 days. Control animals received a sham surgery. Pilot experiments confirmed no differences between a sham surgery and implantation of a saline-infused minipump for cerebral blood flow (CBF) analyses. Systemic infusion of 1000 ng of IL-10 was achieved via a second osmotic minipump filled with human recombinant IL-10 (Sigma-Aldrich, USA), delivering it at a rate of 60 ng/d. The dose was chosen based on a published study examining the effect of exogenous IL-10 on vascular endothelial function and oxidative stress in Ang II-infused mice.[18]

Laser Doppler flowmetry

CBF was monitored by a laser Doppler probe (AD Instruments, USA) placed in a 2 × 2 mm cranial window drilled above the somatosensory cortex. CBF responses to neuronal activity (neurovascular coupling) were examined by three 1-minute whisker stimulations, every 3 minutes. Endothelium-dependent CBF responses were measured after the superfusion of acetylcholine 10 μmol/L (Sigma-Aldrich, USA). Details on the surgical procedure and CBF analysis are available in Data S1.

Blood Pressure

Systolic blood pressure was monitored by tail-cuff plethysmography (Kent Scientific Corp., USA) as detailed in Data S1. Animals were habituated to the procedure 3 days before blood pressure assessment. The measures were taken 24 hours before CBF analysis.

Plasma Cytokine/Chemokine Array

A multiplex bead-based immunoassay (Eve Technologies Corporation, Calgary, AB, Canada) was used for the quantitative determination of 31 mouse plasma cytokines and chemokines, as detailed in Data S1. Given the large number of markers analyzed, a composite inflammatory Z score was computed to obtain a global measure reflecting inflammation and providing a more powered analysis. Before composite calculation and in consultation with an immunologist, cytokines and chemokines were grouped into 4 categories according to their main function: (1) Pro-inflammatory cytokines: IL-1α, IL-6, IL-17, tumor necrosis factor-α (TNF-α) and LIF; (2) Neutrophil chemoattractants: KC (CXCL1), LIX (CXCL5), MIP-2 (CXCL2), and stimulators of their development (G-CSF);

(3) Stimulators of Th1-driven responses: IL-12p40, IL12p70, MIP-1β (CCL4), RANTES (CCL5), MIG (CXCL9), and IP-10 (CXCL10); and (4) Stimulators of Th2 responses: IL-4, IL-5, IL-9, IL-10, IL-13, and MCP-1 (CCL2). The grouping does not intend to reflect the cellular source of each cytokine but rather their main effect as immune mediators. Eotaxin (CCL11) and IL-2 were not classified in any group and are presented independently. The following were not included in the final analysis because of low or no detection in several samples: IL-3, IL-7, interferon-γ, IL-1β, granulocyte-macrophage colony-stimulating factor, macrophage-colony-stimulating factor, vascular endothelial growth factor, and MIP-1α.

A composite score was calculated by converting each marker to a standardized Z score, such that the group mean was zero and the SD was 1. To generate the composite, Z scores within a group were added, as per published methods.[19,20]

Microglia Analysis

Microglia were labeled with the antibody Iba-1 (1:2000, Wako Inc, Richmond, USA), which recognizes a cytoplasmic calcium-binding protein that is expressed in monocytes, and microglia in the brain.[21] Details on the immunohistochemical procedure are available in Data S1. Bright field images were taken with a Leitz Diaplan microscope equipped with an Olympus DP21 camera (Wild Leitz GmbH, Germany). Images were taken from layer V-VI of the somatosensory cortex (8 pictures per section) and from the hippocampal regions CA1, CA3, and DG (2 pictures per region per section). Each 8-bit image was thresholded with the intermodes method and converted to binary with Image J. The "Analyze Particles" function was used to obtain a semiquantitative assessment of the number of microglia/monocytes in the whole micrograph, using a size criterion of 150 pixels.

Superoxide Anion Production

Cortical superoxide production and NADPH oxidase (NOX)-2-derived radicals were measured by lucigenin-enhanced chemiluminescence as detailed in Data S1. Given that lucigenin detects superoxide from various oxidase systems, NOX-2-derived superoxide production was expressed as the percentage of inhibition by gp91ds-tat (a selective NOX-2 inhibitor) relative to the amount of superoxide produced without the inhibitor.

Analysis of Treg Distribution Following Adoptive Transfer

Splenocytes were isolated from C57BL/6 Ly5.1^{+} Foxp3^{GFPki} mice[22] obtained from a colony bred by Dr Ciriaco Piccirillo's laboratory at McGill University. CD25^{+} Treg were isolated using magnetic microbeads (Mitenyi Biotec, USA) following established protocols.[22] Determination of cell purity by flow cytometry indicated an enrichment of 89% Foxp3^{GFP+} on 98% CD25^{+} Treg cells. Adoptive transfer of 3×10^{5} cells was performed as previously described (section Isolation of T lymphocytes and adoptive transfer).

Following adoptive transfer of CD25^{+} Foxp3^{GFP+} cells and after 14 days of Ang II subcutaneous perfusion, mice were anesthetized with sodium pentobarbital (100 mg/kg body weight; CDMV, Canada) and before intracardiac perfusion, inguinal lymph nodes and spleen were dissected. Mice were then perfused with 40 mL PBS, and kidneys and brain were dissected. Purified cell suspensions were then subjected to flow cytometry. Samples were acquired on a LSRII-Fortessa X-20 analyzer (BD Biosciences, USA) and analysis was performed using the FlowJo software v.X (TreeStar, USA), as previously described.[23,24] Characterization of immune cell populations including neutrophils/granulocytes, dendritic cells, B cells, CD3 cells, and natural killer cells has been done with specific clones for each antibody listed in Table S1, following manufacturer recommended dilutions.

Data Analysis and Statistics

Data were analyzed with GraphPad Prism v7.0 (La Jolla, USA). Results are presented as mean±SEM. Multiple group comparisons were evaluated by 1- or 2-way ANOVA, as appropriate, with the Bonferroni correction. For non-normally distributed data, analysis was done with the Kruskal-Wallis test and the Dunn's post hoc correction. A value of $P<0.05$ was considered statistically significant. For each experiment, the statistical test and the precise number of animals are specified in the figure legends.

Results

An overview of the experimental timeline is illustrated in Figure 1.

Effect of Treg on CBF

Adoptive transfer of CD4^{+}CD25^{+} cells (Treg) prevented the disruption of neurovascular coupling (Figure 2A, §$P<0.05$, n=6–9) and of endothelium-dependent dilatation (Figure 2B, §$P<0.05$, n=4–5) caused by chronic Ang II infusion (**$P<0.01$ and *$P<0.05$, respectively). CD4^{+}CD25^{+} T lymphocytes did not elicit changes in cerebrovascular responses in control mice.

We next examined whether the rescue in cerebrovascular responses was correlated with a decrease in systolic blood pressure (SBP). The mean SBP of mice receiving Ang II was significantly higher compared with controls (mean difference

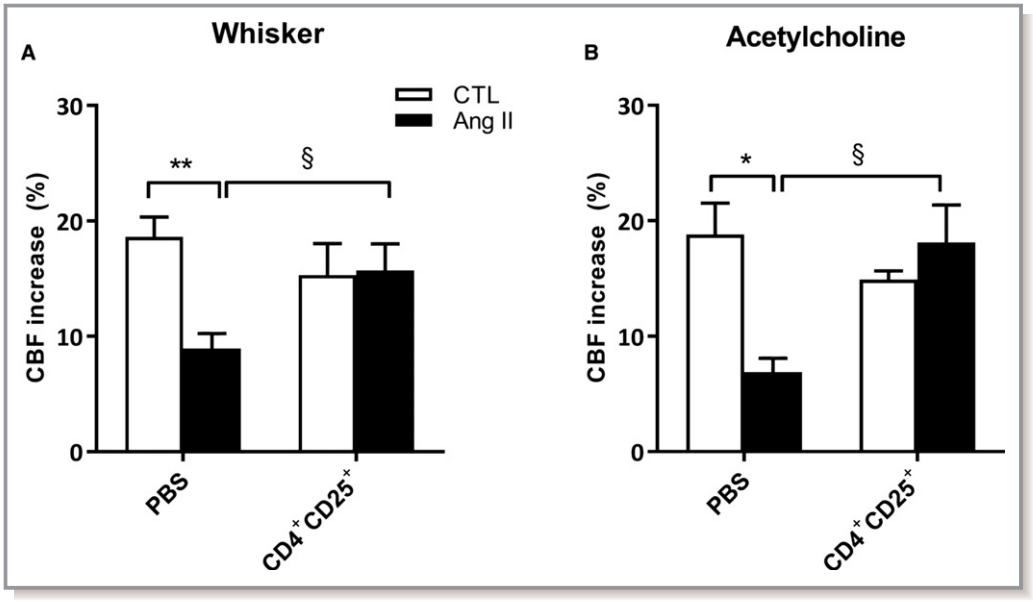

Figure 2. Effect of $CD4^+CD25^+$ regulatory T lymphocytes on CBF. CBF responses to whisker stimulation (**A**) and to the endothelium-dependent vasodilator, acetylcholine (**B**) following adoptive transfer of $CD4^+CD25^+$ cells (3×10^5) or PBS in mice infused s.c. with Ang II (1000 ng/kg per min, 14 d) or in control mice (CTL). Graphs depict the percentage increase in CBF following the stimulation with respect to its initial value, measured by laser Doppler flowmetry. Results represent mean±SEM; n=7 CTL/PBS, n=8 Ang II/PBS, n=6 CTL/$CD4^+CD25^+$ and n=9 Ang II/$CD4^+CD25^+$ mice in (**A**), n=5 CTL/PBS and Ang II/$CD4^+CD25^+$, n=4 Ang II/PBS and CTL/$CD4^+CD25^+$ mice in (**B**). Data were analyzed with 2-way ANOVA followed by Bonferroni correction (§ or $*P<0.05$, $**P<0.01$). Ang II indicates angiotensin II; CBF, cerebral blood flow; CTL, control.

51.5 mm Hg, ¶¶$P<0.0001$, Table S2). Adoptive transfer of 3×10^5 $CD4^+CD25^+$ cells via 2 injections did not result in SBP reduction.

IL-10 Is a Key Mediator of the Cerebrovascular Protective Effect of Treg Cells

IL-10 has been identified as an essential mediator of Treg ($CD4^+CD25^+$) preventing Ang II-induced endothelial dysfunction[18] and reversing brain damage in experimental stroke.[25] To better understand the mechanisms behind the cerebroprotective role of $CD4^+CD25^+$ T cells, we performed adoptive transfer of these cells isolated from mice genetically deficient in IL-10.

In mice receiving Ang II, adoptive transfer of $CD4^+CD25^+$ $Il10^{-/-}$ cells did not rescue neurovascular coupling deficits (Figure 3A), nor did they restore the impaired CBF response to endothelial dilatation (Figure 3B). In control mice, these cells ($CD4^+CD25^+$ $Il10^{-/-}$) importantly attenuated the response to whisker stimulation (Figure 3A, ####$P<0.0001$, n=5–9), and a similar trend was seen in response to acetylcholine (Figure 3B, $P=0.095$, n=5–6). Despite affecting cerebrovascular responses, 2 injections of $CD4^+CD25^+Il10^{-/-}$ cells did not have an effect on SBP in naïve animals (Table S2).

IL-10 Rescues the Neurovascular Uncoupling Induced by Ang II

We examined whether IL-10 itself is capable of preventing the cerebrovascular dysfunctions caused by Ang II. Exogenous IL-10 administration resulted in a 2-fold increase in CBF upon whisker stimulation in Ang II-infused mice when compared with mice only receiving Ang II (mean CBF increase 16.4% versus 8.4%; Figure 4A, ****$P<0.0001$, n=6–12). IL-10 administration did not increase neurovascular coupling responses in control animals beyond normal levels. Although the attenuation of endothelial responses caused by Ang II (****$P<0.0001$) did not significantly recover with exogenous IL-10 infusion, there was a trend for a 1.6-fold increase in CBF with IL-10 administration (mean CBF increase 11.8% Ang II + IL-10 versus 7.3% Ang II; Figure 4B, $P=0.065$, n=6–11). IL-10 administration did not result in a decrease in SBP in mice infused with Ang II (Table S3).

Adoptive Transfer of Treg Cells Prevents Systemic Immune Responses Induced by Ang II

An array of immune mediators was examined in plasma. There was a trend revealing higher levels of the composite score involving pro-inflammatory cytokines, such as IL-1α,

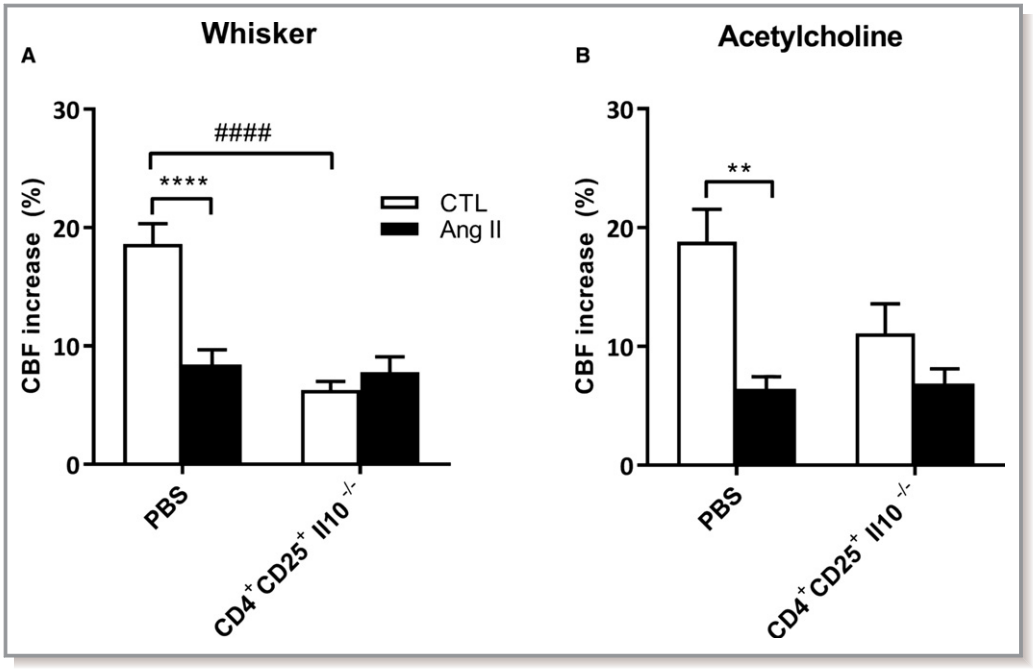

Figure 3. IL-10 is a key mediator of the cerebrovascular protective effect of $CD4^+CD25^+$ regulatory T cells. CBF responses to whisker stimulation (**A**) and to acetylcholine (**B**) following adoptive transfer of $CD4^+CD25^+$ cells (3×10^5) isolated from mice lacking the gene for IL-10. $CD4^+CD25^+$ *Il10*$^{-/-}$ or PBS injections were given to mice infused s.c. with Ang II (1000 ng/kg per min, 14 d) or to control mice (CTL). Graphs depict the percentage increase in CBF following the stimulation with respect to its initial value, measured by laser Doppler flowmetry. Results represent mean±SEM; n=7 CTL/PBS, n=9 Ang II/PBS and CTL/$CD4^+CD25^+$ *Il10*$^{-/-}$ and n=5 Ang II/$CD4^+CD25^+$ *Il10*$^{-/-}$ mice in (**A**), n=5 CTL/PBS, Ang II/PBS and Ang II/$CD4^+CD25^+$ *Il10*$^{-/-}$ and n=6 CTL/$CD4^+CD25^+$ *Il10*$^{-/-}$ mice in (**B**). Data were analyzed with 2-way ANOVA followed by Bonferroni correction (**P<0.01, **** or ####P<0.0001). Ang II indicates angiotensin II; CBF, cerebral blood flow; CTL, control mice; IL-10, interleukin-10.

IL-6, LIF, and TNF-α, in animals receiving Ang II compared with controls (Figure 5A, P=0.115, n=4–11; Figure S1 for individual cytokines). Composite scores of pro-inflammatory cytokines tended to be lower following adoptive transfer of $CD4^+CD25^+$ cells (Figure 5A, P=0.072), in particular reflecting attenuated levels of IL-1α, IL-6, and IL-17. Ang II also led to an increase in the composite score reflecting plasma neutrophil chemoattractants, such as LIX (CXCL5) and MIP-2 (CXCL2) as well as G-CSF (Figure 5B, *P<0.05, n=4–11 and Figure S2). This increase was also attenuated by adoptive transfer of $CD4^+CD25^+$ cells (*P<0.05). In addition, Ang II led to an increase in the composite score of mediators of Th1 responses, such as IL-12 and MIG (CXCL9), but $CD4^+CD25^+$ T cells did not significantly attenuate this effect (Figure 5C, n=4–11 and Figure S3).

The inflammatory profile of hypertensive mice receiving $CD4^+CD25^+$ *Il10*$^{-/-}$ cells tended to be different from that of mice receiving wild-type $CD4^+CD25^+$ cells (Figure 5 and Figures S1 through S3). For the composite score of pro-inflammatory mediators, the mean Z score for the Ang II + $CD4^+CD25^+$ *Il10*$^{-/-}$ group was higher compared with that of Ang II + $CD4^+CD25^+$ (mean 0.245±0.2 versus −0.365±0.1), although after Bonferroni or Dunn's post hoc correction these differences remained as trends, and likewise for the neutrophil and Th1 composite score.

Neither Ang II nor $CD4^+CD25^+$ adoptive transfer had a significant impact on the composite score reflecting cytokines and chemokines that stimulate Th2 responses (Figure 5D). However, individually, the plasma levels of IL-10 and IL-13 tended to be higher than controls in mice receiving Ang II (Figure S4). There were also no significant differences in eotaxin (CCL11) and IL-2 levels between groups (Figure S5).

Given that $CD4^+CD25^+$ *Il10*$^{-/-}$ cells significantly impaired neurovascular coupling in naïve mice, we examined whether this effect could be correlated to the pattern of inflammatory mediators found in the peripheral blood of recipient mice. In line with the CBF results, the plasma profile of naïve mice receiving $CD4^+CD25^+$ *Il10*$^{-/-}$ cells significantly differed from that of mice receiving wild-type $CD4^+CD25^+$ cells or PBS. They showed a higher composite score reflecting increased expression of pro-inflammatory cytokines (Figure 6A, *P<0.05, n=4–11 and Figure S6), as well as higher composite scores reflecting increased levels of Th1

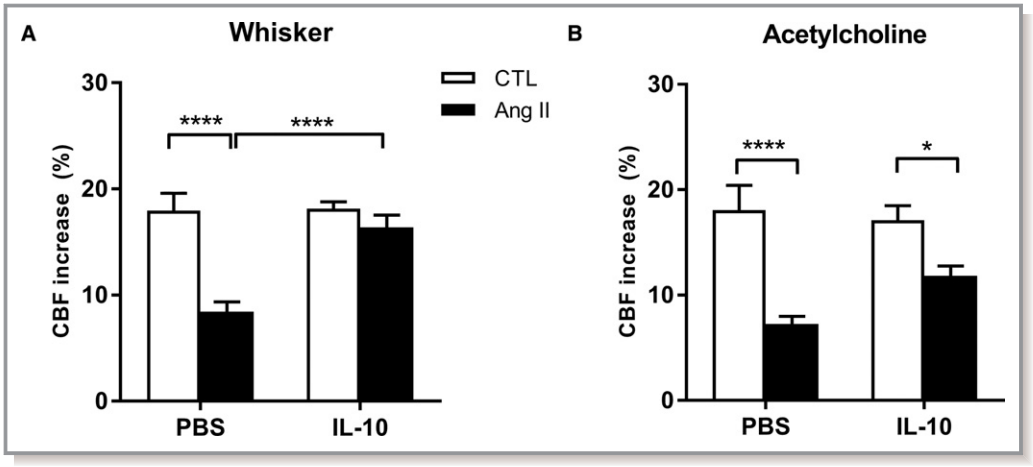

Figure 4. IL-10 rescues the neurovascular coupling deficit induced by Ang II. CBF responses to whisker stimulation (**A**) and to acetylcholine (**B**) following simultaneous administration of Ang II (1000 ng/kg per min) and IL-10 (60 ng/d) or Ang II or IL-10 alone for 14 d. Graphs depict the percentage increase in CBF following the stimulation with respect to its initial value, measured by laser Doppler flowmetry. Results represent mean±SEM; n=8 CTL/PBS, n=12 Ang II/PBS, n=6 CTL/IL-10, and n=11 Ang II/IL-10 mice in (**A**), n=6 CTL/PBS and CTL/IL-10, n=8 Ang II/PBS, and n=11 Ang II/IL-10 mice in (**B**). Data were analyzed by 2-way ANOVA followed by Bonferroni correction (*P<0.05 and ****P<0.0001). Ang II indicates angiotensin II; CBF, cerebral blood flow; CTL, control; IL-10, interleukin-10.

stimulators (Figure 6C, *P<0.05, n=4–11 and Figure S7). There was a trend showing higher composite scores reflecting cytokines involved in neutrophil trafficking (Figure 6B, P=0.108 Kruskal-Wallis test, n=4–11 and Figure S8) and no significant differences in the composite score reflecting stimulators of Th2 responses between groups (Figure 6D and Figure S9).

Effect of Treg Cells on Cerebral Gliosis and NOX-2-Derived Superoxide Radicals

Given the protective role of $CD4^+CD25^+$ Treg cells on CBF, and the recent evidence that Ang II induces hippocampal microgliosis,[26] we examined whether $CD4^+CD25^+$ adoptive transfer would attenuate the inflammatory effects of Ang II beyond the periphery. Mice receiving Ang II exhibited a significantly higher number of Iba-1+ cells compared with controls, both in the somatosensory cortex, where cerebrovascular responses were examined, and in the hippocampus (Figure 7A, *P<0.05 and **P<0.01, respectively). $CD4^+CD25^+$ T cells prevented the increase in Iba-1+ cells in both regions (*P<0.05 and ***P<0.0001, n=3–5).

We further examined the cerebral production of superoxide. Ang II infusion led to a significant increase in superoxide radicals in the brain cortex, and adoptive transfer of $CD4^+CD25^+$ cells prevented this effect (Figure 7B, *P<0.05, n=4–9). Injection of $CD4^+CD25^+$ cells derived from *Il10* knockout mice led to a similar effect (Figure 7B, P=0.057).

To quantify NOX-2-derived superoxide radicals (the main NOX isoform present in brain vessels[14]), cortical tissue was incubated with gp91ds-tat, a selective NOX-2 inhibitor. As seen in Figure 7C, gp91ds-tat inhibited superoxide production to a greater extent in the brain of Ang II-infused mice compared with controls, indicating increased NOX-2-derived radicals because of Ang II (Figure 7C, *P<0.05, n=3–8). In animals receiving $CD4^+CD25^+$ or $CD4^+CD25^+$ *Il10*$^{-/-}$ cell injections, mean NOX-2-derived superoxide anion production was not significantly different from animals receiving only Ang II.

Treg Distribution

Interestingly, analysis of Treg distribution following adoptive transfer revealed that after 2 injections of 3×10^5 cells, only a negligible number of adoptively transferred Treg were detected in brain, while much higher levels were found in other tissues such as the kidneys, inguinal lymph nodes, and spleen (Figure S10). In addition, the total number of endogenous myeloid and lymphoid cells (neutrophils/granulocytes, dendritic cells, B cells, $CD3^+$ cells, and natural killer cells) quantified from the brain was the same in mice receiving Ang II and Treg compared with controls receiving Treg (Figure S11).

Discussion

This study shows for the first time a role for the adaptive immune system in modulating cerebrovascular responses. Our major new findings are that $CD4^+CD25^+$ T cells, commonly identified as Treg,[2,9,10,18] exhibit a neuroprotective role with respect to the cerebrovascular, inflammatory, and

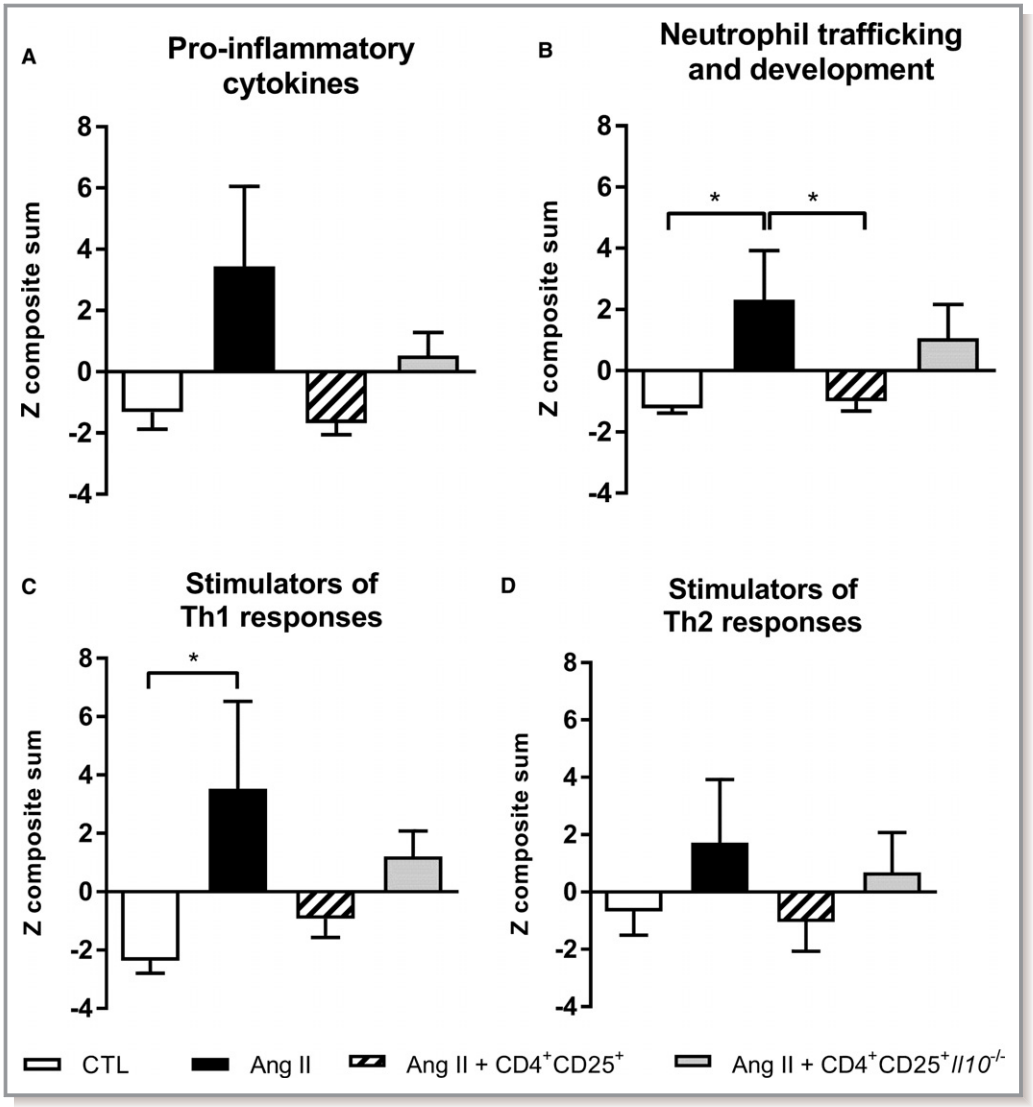

Figure 5. $CD4^+CD25^+$ regulatory T cells prevent systemic immune responses induced by Ang II. Analysis of plasma cytokines and chemokines following adoptive transfer of $CD4^+CD25^+$ or $CD4^+CD25^+$ $Il10^{-/-}$ cells (3×10^5) in mice infused s.c. with Ang II (1000 ng/kg per min, 14 d) and in control mice (CTL). Cytokines were grouped into 4 categories: pro-inflammatory cytokines (IL-1α, IL-6, IL-17, TNF-α, and LIF) (**A**), neutrophil chemoattractants (KC, LIX, MIP-2) and stimulators of their development (G-CSF) (**B**), stimulators of Th1-driven responses (IL-12p40, IL12p70, MIP-1β, RANTES, MIG, and IP-10) (**C**), and stimulators of Th2 responses (IL-4, IL-5, IL-9, IL-10, IL-13, and MCP-1) (**D**). A composite score was calculated by converting each marker to a standardized Z score and then added. Results represent mean±SEM; n=11 CTL, n=7 Ang II and Ang II+ $CD4^+CD25^+$, n=4 Ang II+ $CD4^+CD25^+$ $Il10^{-/-}$ mice. *P<0.05, by Kruskal-Wallis and Dunn's post hoc correction (**A**, **C**, **D**) or 1-way ANOVA followed by Bonferroni correction (**B**). Ang II indicates angiotensin II; CTL, control mice; G-CSF, granulocyte colony-stimulating factor; IL, interleukin; IP-10, Interferon gamma-induced protein 10; KC, Keratinocyte chemoattractant; LIF, Leukemia inhibitory factor; LIX, lipopolysaccharide (LPS)-induced CXC chemokine; MCP, Monocyte chemoattractant protein; MIG, Monokine induced by gamma interferon; MIP, Macrophage Inflammatory Protein; RANTES, Regulated on activation, normal T cell expressed and secreted; TNF, tumor necrosis factor.

oxidative injury induced by Ang II in the brain. To the best of our knowledge, this is the first in vivo study to examine the functional role of $CD4^+CD25^+$ T lymphocytes in the regulation of CBF in Ang II-induced hypertension.

In our study, we identified IL-10 as a key regulator of the cerebrovascular protective role of $CD4^+CD25^+$ T cells. First, we showed that $CD4^+CD25^+$ cells isolated from mice genetically devoid of IL-10 lost their protective effect to Ang

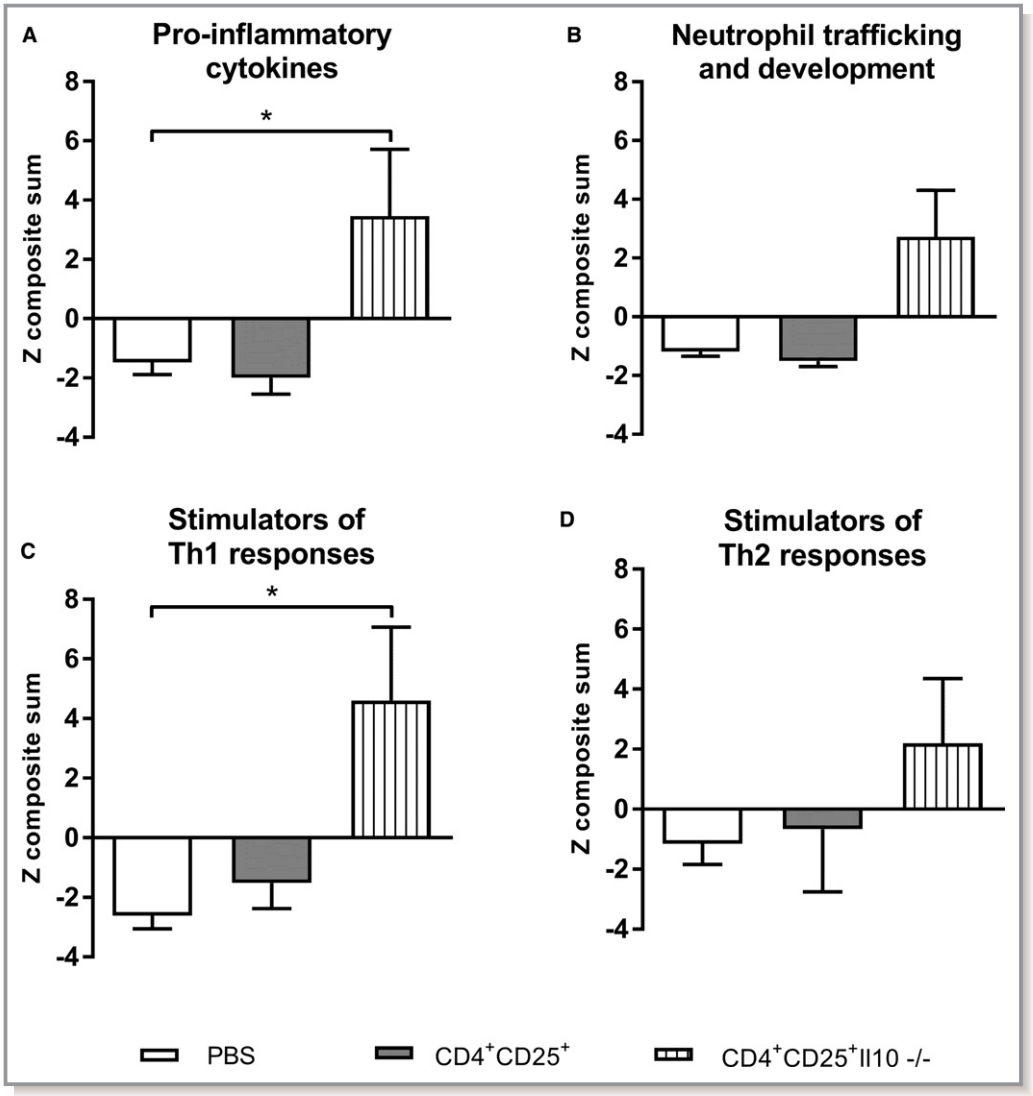

Figure 6. $CD4^+CD25^+$ *Il10*$^{-/-}$ cells affect systemic immune responses in naïve mice. Analysis of plasma cytokines and chemokines following adoptive transfer of $CD4^+CD25^+$ or $CD4^+CD25^+$ *Il10*$^{-/-}$ cells (3×10^5) or PBS to naïve mice. Cytokines were grouped into 4 categories: pro-inflammatory cytokines (IL-1α, IL-6, IL-17, TNF-α, and LIF) (**A**), neutrophil chemoattractants (KC, LIX, MIP-2) and stimulators of their development (G-CSF (**B**)), stimulators of Th1 responses (IL-12p40, IL12p70, MIP-1β, RANTES, MIG, and IP-10) (**C**), and stimulators of Th2 responses (IL-4, IL-5, IL-9, IL-10, IL-13 and MCP-1) (**D**). A composite score was calculated by converting each marker to a standardized Z score and then added. Results represent mean±SEM; n=11 PBS, n=4 $CD4^+CD25^+$ and n=7 $CD4^+CD25^+$ *Il10*$^{-/-}$ mice. *P<0.05 by 1-way ANOVA followed by Bonferroni correction (**A**, **D**) or Kruskal-Wallis followed by Dunn's post hoc correction (**B**, **C**). G-CSF, granulocyte colony-stimulating factor; IL, interleukin; IP-10, Interferon gamma-induced protein 10; KC, Keratinocyte chemoattractant; LIF, Leukemia inhibitory factor; LIX, lipopolysaccharide (LPS)-induced CXC chemokine; MCP, Monocyte chemoattractant protein; MIG, Monokine induced by gamma interferon; MIP, Macrophage Inflammatory Protein; RANTES, Regulated on activation, normal T cell expressed and secreted; TNF, tumor necrosis factor.

Il-induced cerebrovascular damage. Second, we demonstrate that recombinant IL-10 itself is capable of antagonizing the injurious actions of Ang II on neurovascular coupling. A protective role for IL-10 has been identified in other studies. Using genetic or pharmacological approaches to deplete IL-10 derived from Treg, Kassan and colleagues showed that IL-10 is critical to prevent endothelial dysfunction and oxidative stress in mesenteric arteries damaged by Ang II.[18] In the brain, Liesz et al further found that mice receiving IL-10-deficient Treg had larger infarct volumes than mice receiving normal Treg in a model of experimental ischemia.[25] This should not imply that circulating IL-10 exerts its effects

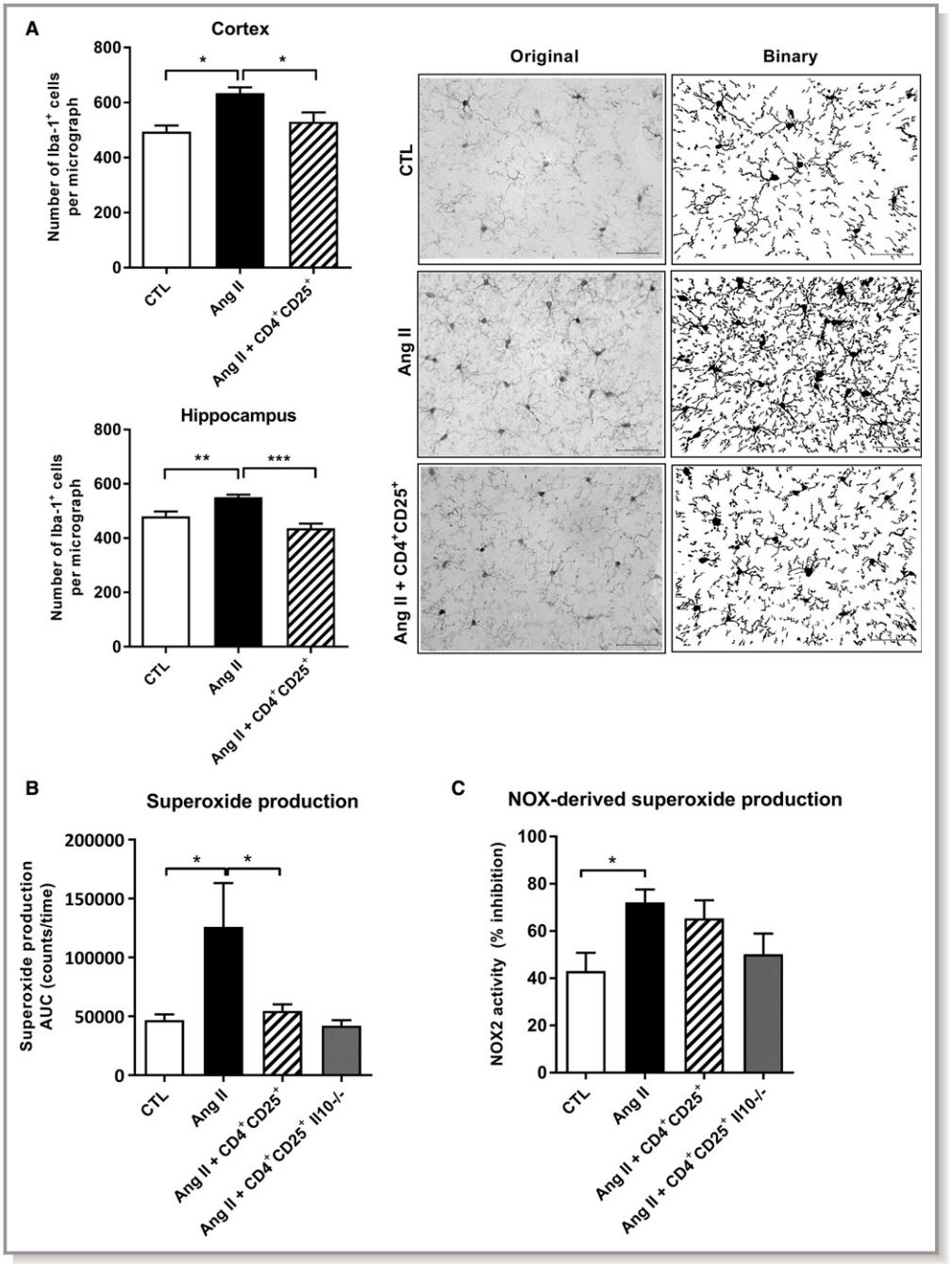

Figure 7. Effect of $CD4^+CD25^+$ regulatory T cells on cerebral gliosis and oxidative stress. **A,** Microglia/monocytes were stained and visualized with Iba-1. A semiquantitative assessment of the number of Iba-1+ cells per micrograph was performed in the somatosensory cortex and hippocampus. Representative micrographs are shown. Scale bar=50 µm. Graphs represent mean±SEM; n=3 CTL and Ang II, n=5 Ang II+$CD4^+CD25^+$ mice, **P*<0.05, by 1-way ANOVA followed by Bonferroni correction (cortex) or ***P*<0.01, ****P*<0.001 by Kruskal-Wallis test followed by Dunn's post hoc correction (hippocampus). **B,** Superoxide anion production was measured by lucigenin-enhanced chemiluminescence of cortical tissue incubated with NADPH and extrapolated from the area under the curve (AUC) counts/time. Graphs represent mean±SEM; n=6 CTL n=7 Ang II, n=9 Ang II+$CD4^+CD25^+$ and n=4 Ang II+$CD4^+CD25^+$ *Il10*$^{-/-}$ mice, **P*<0.05, by 1-way ANOVA followed by Bonferroni correction. **C,** Cerebral NOX-2-derived radicals were determined based on the extent of the inhibition of superoxide anion production following the addition of its specific inhibitor, gp91ds-tat. Graphs represent mean± SEM (n=5 CTL, n=7 Ang II, n=8 Ang II+$CD4^+CD25^+$ and n=3 Ang II+$CD4^+CD25^+$ *Il10*$^{-/-}$ mice, **P*<0.05, by 1-way ANOVA followed by Bonferroni. Ang II indicates angiotensin II; CTL, control; NOX, NADPH oxidase.

directly on tissues, or that circulating IL-10 is the sole important cytokine acting in Treg-mediated neuroprotection. Indeed, our study shows that $CD4^+CD25^+$ T cells modulate a large repertoire of plasmatic cytokines, suggesting that Treg could prevent CBF impairments by modulation of the global immune profile. This observation is reinforced by the finding that $CD4^+CD25^+$ T cells isolated from *Il10* knockouts still prevented the increase in cortical superoxide anion production induced by Ang II while losing their protective effect on CBF. This could suggest that although oxidative stress may be able to disrupt CBF regulation, additional pathological processes that follow in consequence, such as inflammation, could also have a prominent role later on. This could also explain why antioxidant treatment has not proven efficacious to control blood pressure in hypertensive patients,[27] where multiple pathological processes affect CBF in parallel.

In line with this, although cerebral endothelial responses were modulated with exogenous IL-10, the differences were not significant, suggesting that the infusion of IL-10 did not fully reproduce the protective effect of adoptively transferred $CD4^+CD25^+$ T cells. It is possible that other anti-inflammatory factors secreted by Treg, such as transforming growth factor-β and IL-35,[28] or the attenuation of pro-inflammatory immune pathways, are needed to fully mimic the protective effect of Treg on the brain endothelium. It is also possible that upon tissue injury endothelial cells are less responsive to IL-10 compared with other cells in the neurovascular unit. Indeed, Gonzalez and colleagues have shown that although endothelial cells express the IL-10 receptor in physiological conditions, with excitotoxic injury IL-10 receptor immunoreactivity increases to maximal levels in reactive astrocytes and microglia.[29] Therefore, although in normal conditions endothelial cells can respond to IL-10, in the presence of tissue damage (eg, caused by Ang II) they could be outcompeted by other cells expressing higher levels of the IL-10 receptor, which could explain the recovery of neurovascular coupling but not of endothelial dilatory responses.

In the present study, we also found that the positive effect of $CD4^+CD25^+$ cells on CBF was not accompanied by a decrease in SBP. Such response fits with the finding that Ang II impairs neurovascular coupling and cerebral endothelial function independently of its hypertensive effect.[30] Indeed, the injurious actions of slow pressor concentrations of Ang II on the cerebral microcirculation are mediated through activation of the Ang type 1 (AT_1) receptor and the production of superoxide radicals derived from NADPH oxidase, and occur before the increased in blood pressure.[14,15] In support, infusion of phenylephrine, which increases blood pressure to the same level of a dose of 1000 ng/kg per minute of Ang II but independently of the renin–angiotensin system, does not disrupt neurovascular coupling.[14]

Although in the experimental conditions of our study we did not see an effect of $CD4^+CD25^+$ cells attenuating hypertension, we found that they prevented the increase in cerebral superoxide radicals induced by Ang II, which is in line with the recovery of cerebrovascular responses. We do not deny that Treg could reduce blood pressure, because other studies demonstrated such an effect.[9,18] However, differences in adoptive transfer protocols (3 and 6 injections, versus 2 in our study) could explain the different result. We also cannot deny the possibility that $CD4^+CD25^+$ cells modulated the development of hypertension in our model but that the final blood pressure at the end of the study was not different.

Likewise, the lack of effect of Treg on diminishing NOX-2 superoxide radicals could indicate that Treg may reduce superoxide production either by acting on other NOX isoforms that are also expressed in brain, such as NOX-1,[31] or through other oxidase systems, such as xanthine oxidase, mitochondrial electron transport, cyclo-oxygenase, NO synthase, and lipo-oxygenase, some of which are also known to be affected by hypertension.[32] Given that expression of NADPH oxidases has been found in multiple brain cells including neurons, microglia, and astrocytes,[33,34] as well as in cells of the brain vasculature,[35] future studies could use pharmacological (ie, using NOX-specific inhibitors) or genetic strategies (ie, NOX-specific knockout mice) to investigate the enzymatic source(s) by which Treg diminish superoxide production in the brain cortex and in isolated cerebral vessels.

Besides diminishing superoxide production and systemic inflammation, $CD4^+CD25^+$ cells prevented the increase in microglia induced by Ang II. The mechanisms linking Treg and microglia could be several and complementary. Considering the damage to the blood–brain barrier induced by Ang II[36], it is possible that following adoptive transfer, Treg or cytokines produced by them traffic to the brain where they directly interact with microglia. Indeed, Treg infiltration to the brain parenchyma has been reported in stroke models,[37] where blood–brain barrier breakdown also occurs. The infiltrated T cells were key sources of the inflammatory cytokine interferon-γ, which could activate microglia.[38] It has also been shown that Treg can alter the proteome of cultured microglial cells, both by direct cell-to-cell contact and via the release of IL-10 and transforming growth factor-β, diminishing pro-inflammatory cytokines and proteins that regulate cell motility.[39] At the same time, the immunosuppressive actions of Treg in the periphery could diminish the infiltration of immune cells (T cells, monocytes/macrophages, and neutrophils) into the brain, preventing injury and thus indirectly impacting on microglia responses. The antagonizing effect of Treg on microglia numbers is not exclusive to our hypertension model; it has also been observed in murine models of HIV-encephalitis,[40] Parkinson's disease,[39] and cerebral

ischemia.[41] Given the recent finding that Ang II affects hippocampal microglia phenotype towards an inflammatory, active metabolic state,[26] it would be of interest to investigate whether Treg also modulate microglia morphologic activation, state of surveillance, and extracellular digestion, besides diminishing microglia numbers.

An intriguing finding was the observation of impaired neurovascular coupling with administration of $CD4^+CD25^+$ $Il10^{-/-}$ cells into controls. We reasoned that this could be related to a phenotypic change of these cells because of exposure to the pro-inflammatory microenvironment in the knockout mice, which exhibit increased IL-6, TNF-α, and IL1-β in serum as well as intestinal inflammation.[42] Indeed, it is known that Treg could exhibit functional plasticity when exposed to an inflammatory microenvironment, reprogramming into nonsuppressive, cytokine-producing effector cells that contribute to tissue damage.[22] Supporting this, analysis of plasma cytokines of naïve mice that received $CD4^+CD25^+$ cells from $Il10^{-/-}$ donors revealed an inflammatory pattern of immune mediators, involving upregulation of cytokines such as IL-6, IL-17, LIF, TNF-α, IL-10, IL-12, IL-13, and the chemokines MIP1-β (CCL4), RANTES (CCL5), KC (CXCL1), and MIP-2 (CXCL2). The implications of these findings are 2-fold. First, they are consistent with the deficits in neurovascular coupling caused by $CD4^+CD25^+$ $Il10^{-/-}$ cells in naïve animals. Second, they open up a new hypothesis suggesting that CBF is highly sensitive to pro-inflammatory cytokines. In this regard, it was intriguing that plasmatic IL-10 levels were elevated in naïve mice receiving Ang II or $CD4^+CD25^+$ $Il10^{-/-}$ cells and that exhibited cerebrovascular deficits. Since immune responses are tightly balanced, a possible explanation is that the pro-inflammatory milieu resulting from $CD4^+CD25^+$ $Il10^{-/-}$ adoptive transfer and from Ang II activates compensatory pathways in the recipient that lead to IL-10 production. Indeed, it has been previously observed that Ang II infusion causes an increase in plasmatic IL-10 along with the rise of pro-inflammatory cytokines, both of which are diminished by Treg transfer.[9] Another possibility is that plasma cytokines do not reflect concentrations those in tissues. This has been observed in a model of Ang II-induced hypertension, where blood and spleen IL-10 concentrations were lower in mice receiving Ang II compared with their controls, while IL-10 levels were higher in kidney and aorta.[43]

The ample repertoire of cytokines and chemokines induced by Ang II and modulated by Treg adoptive transfer warrants future investigations. The plasma elevations in IL-6 and TNF-α are interesting in view of earlier findings showing elevations of these cytokines in different brain regions, such as the paraventricular nucleus of the hypothalamus and the hippocampus,[26,44] highlighting the potential for cross-talk between peripheral and brain-derived immune mediators. Likewise, the attenuation of IL-17 upon Treg adoptive transfer could suggest an involvement of this cytokine in CBF regulation, a hypothesis supported by previous studies showing its involvement in the development of hypertension, endothelial dysfunction, and cognitive impairment.[45–47]

A number of questions merit discussion. An aspect that requires elucidation is whether $CD4^+CD25^+$ cells prevent trafficking of other immune cells to the brain in our Ang II model. We have examined $CD4^+CD25^+$ cell localization showing that following adoptive transfer of 3×10^5 cells (2 injections) only a negligible amount of exogenous Treg was detected in the brain, while significantly penetrating other tissues such as the kidneys, inguinal lymph nodes, and spleen. In addition, there were no differences in the total number of brain myeloid cells, B cells, natural killer cells, or $CD3^+$ cells in mice receiving Ang II + Treg compared with controls. These results would suggest that exogenous Treg prevent the negative effects of Ang II on CBF and microglia activation by preventing the entry of immune mediators through the blood–brain barrier, and/or by regulating other mechanisms from the luminal side. These findings are in line with the study of Li and colleagues, who showed that the protective effect of Treg on reducing poststroke inflammation and blood–brain barrier dysfunction is conferred without penetration of exogenous Treg to the brain parenchyma but rather by modulation of peripheral immune cell populations.[48] This should not rule out that trafficking of immune cells to the brain does not occur in hypertension models. Indeed, in Ang II-induced hypertension models, accumulation of immune cells ($CD3^+$, macrophages, and leukocytes) into the cerebral artery wall has been observed,[36,49,50] and bone marrow–derived cells have been found in the paraventricular nucleus of naive Sprague–Dawley rats challenged with a continuous infusion of Ang II,[51] suggesting that immune cells can penetrate the brain parenchyma in this model.

Interestingly, several studies from different disciplines have shown that Treg can prevent the infiltration of immune cells to cerebral sites. For example, Baruch and collaborators reported that in a transgenic mouse model of Alzheimer disease—which shares similarities to our hypertension model by being characterized by a chronic low-grade inflammation—transient depletion of Treg increased the recruitment of immune cells to the brain, particularly monocytes and $CD4^+$ T cells, including Treg.[52] In more aggressive models of inflammation, this phenomenon has also been observed (for instance, in models of viral encephalitis[53] and glioma,[54]) where Treg were found to prevent infiltration of T lymphocytes, granulocytes, and macrophages with phagocytic activity to the brain parenchyma and cerebral microvasculature.

Furthermore, it would be interesting to examine whether the phenotype of $CD4^+CD25^+$ cells (markers expressed, mediators released) changes because of Ang II. Answering

this question would help to better understand how the repertoire of inflammatory mediators changes in recipient mice receiving Ang II and $CD4^+CD25^+$ cells. Finally, given that Treg adoptive transfer was performed in mice with competent immune systems, it remains to be demonstrated whether Treg cells alone are sufficient to mitigate Ang II-induced cerebrovascular damage, or whether other immune cells are also needed. Recent evidence in the periphery would support the first possibility, as *Rag1-/-* mice, which lack T and B lymphocytes, have blunted increases in systolic blood pressure, mesenteric artery stiffness, and vascular remodeling when infused with Ang II and adoptively transferred with Treg.[55]

Taken together, our findings suggest that modulating the immune system and targeting inflammation in hypertension could be a promising approach for reducing damage to end-organs, particularly the brain. Given that hypertension and chronic inflammation have been associated as important risk factors for stroke, cognitive impairment, and dementia, the results of this study could open the door for future investigations to examine the influence of the immune system and inflammation on the cerebral circulation and brain degeneration.

Conclusions

This study is the first demonstration that $CD4^+CD25^+$ T lymphocytes modulate CBF and the cerebrovascular injury induced by Ang II. Besides abrogating impairments in neurovascular coupling and cerebral endothelial dilatory responses, adoptive transfer of $CD4^+CD25^+$ T cells prevented peripheral inflammation, cerebral gliosis, and oxidative stress in the brain.

Acknowledgments

The authors would like to thank Dr Sylvie Lesage (Centre de recherche de l'Hôpital Maisonneuve-Rosemont, Canada) for providing *Il10*$^{-/-}$ mice, Dr Jean-François Gauchat (Université de Montréal, Canada) for guidance with the classification of immune mediators, and Dr Simon Allard (John Hopkins University, USA) for assistance with microglia quantification.

Sources of Funding

Girouard was supported by the Canadian Institutes of Health Research (CIHR, MOP285902), the Fonds de recherche du Québec—Santé (FRQS), the Heart and Stroke Foundation of Canada (HSFC), and the Canada Foundation for Innovation (CFI). Schiffrin received support from CIHR (102606, 123465 and 143348), from a Canada Research Chair on Hypertension and Vascular Research, and from the CFI. Piccirillo was supported by the CIHR (MOP67211 and MOP84041). Iulita received support from the Herbert H. Jasper Postdoctoral Research Fellowship in Neurosciences, Université de Montréal (2016–2017), and from a Bourse Postdoctorale from FRQS. Duchemin received support from the Heart and Stroke Foundation of Canada. Barhoumi received support from a Bourse Postdoctorale from the Société québécoise d'hypertension artérielle (SQHA) and from the McGill University Richard and Edith Strauss Postdoctoral Fellowship. Istomine was the holder of a FRQS Doctoral Fellowship. Laurent obtained a postdoctoral award from Fondation pour l'Aide à la Recherche sur la Sclérose en Plaques (ARSEP) (France) and the FRQS and currently holds a fellowship from the Canadian Institutes of Health Research.

Disclosures

None.

References

1. Idris-Khodja N, Mian MO, Paradis P, Schiffrin EL. Dual opposing roles of adaptive immunity in hypertension. *Eur Heart J*. 2014;35:1238–1244.
2. Pyzik M, Piccirillo CA. TGF-beta1 modulates Foxp3 expression and regulatory activity in distinct CD4+ T cell subsets. *J Leukoc Biol*. 2007;82:335–346.
3. Tang Q, Bluestone JA. The Foxp3+ regulatory T cell: a jack of all trades, master of regulation. *Nat Immunol*. 2008;9:239–244.
4. Chaudhry A, Samstein RM, Treuting P, Liang Y, Pils MC, Heinrich JM, Jack RS, Wunderlich FT, Bruning JC, Muller W, Rudensky AY. Interleukin-10 signaling in regulatory t cells is required for suppression of Th17 cell-mediated inflammation. *Immunity*. 2011;34:566–578.
5. Grossman WJ, Verbsky JW, Barchet W, Colonna M, Atkinson JP, Ley TJ. Human T regulatory cells can use the perforin pathway to cause autologous target cell death. *Immunity*. 2004;21:589–601.
6. Tadokoro CE, Shakhar G, Shen S, Ding Y, Lino AC, Maraver A, Lafaille JJ, Dustin ML. Regulatory T cells inhibit stable contacts between CD4+ T cells and dendritic cells in vivo. *J Exp Med*. 2006;203:505–511.
7. Kvakan H, Kleinewietfeld M, Qadri F, Park JK, Fischer R, Schwarz I, Rahn HP, Plehm R, Wellner M, Elitok S, Gratze P, Dechend R, Luft FC, Muller DN. Regulatory T cells ameliorate angiotensin ii-induced cardiac damage. *Circulation*. 2009;119:2904–2912.
8. Matrougui K, Abd Elmageed Z, Kassan M, Choi S, Nair D, Gonzalez-Villalobos RA, Chentoufi AA, Kadowitz P, Belmadani S, Partyka M. Natural regulatory T cells control coronary arteriolar endothelial dysfunction in hypertensive mice. *Am J Pathol*. 2011;178:434–441.
9. Barhoumi T, Kasal DA, Li MW, Shbat L, Laurant P, Neves MF, Paradis P, Schiffrin EL. T regulatory lymphocytes prevent angiotensin II-induced hypertension and vascular injury. *Hypertension*. 2011;57:469–476.
10. Kasal DA, Barhoumi T, Li MW, Yamamoto N, Zdanovich E, Rehman A, Neves MF, Laurant P, Paradis P, Schiffrin EL. T regulatory lymphocytes prevent aldosterone-induced vascular injury. *Hypertension*. 2012;59:324–330.
11. Iadecola C, Park L, Capone C. Threats to the mind: aging, amyloid, and hypertension. *Stroke*. 2009;40:S40–S44.
12. Xie Y, Mies G, Hossmann KA. Ischemic threshold of brain protein synthesis after unilateral carotid artery occlusion in gerbils. *Stroke*. 1989;20:620–626.
13. Jennings JR, Muldoon MF, Ryan C, Price JC, Greer P, Sutton-Tyrrell K, van der Veen FM, Meltzer CC. Reduced cerebral blood flow response and compensation among patients with untreated hypertension. *Neurology*. 2005;64:1358–1365.
14. Kazama K, Anrather J, Zhou P, Girouard H, Frys K, Milner TA, Iadecola C. Angiotensin II impairs neurovascular coupling in neocortex through NADPH oxidase-derived radicals. *Circ Res*. 2004;95:1019–1026.
15. Girouard H, Park L, Anrather J, Zhou P, Iadecola C. Angiotensin ii attenuates endothelium-dependent responses in the cerebral microcirculation through Nox-2-derived radicals. *Arterioscler Thromb Vasc Biol*. 2006;26:826–832.
16. Girouard H, Lessard A, Capone C, Milner TA, Iadecola C. The neurovascular dysfunction induced by angiotensin ii in the mouse neocortex is sexually dimorphic. *Am J Physiol Heart Circ Physiol*. 2008;294:H156–H163.

17. Barhoumi T, Paradis P, Mann KK, Schiffrin EL. Isolation of immune cells for adoptive transfer. *Methods Mol Biol*. 2017;1527:321–344.
18. Kassan M, Galan M, Partyka M, Trebak M, Matrougui K. Interleukin-10 released by CD4(+)CD25(+) natural regulatory T cells improves microvascular endothelial function through inhibition of NADPH oxidase activity in hypertensive mice. *Arterioscler Thromb Vasc Biol*. 2011;31:2534–2542.
19. Hopkins MH, Flanders WD, Bostick RM. Associations of circulating inflammatory biomarkers with risk factors for colorectal cancer in colorectal adenoma patients. *Biomark Insights*. 2012;7:143–150.
20. Morrison L, Laukkanen JA, Ronkainen K, Kurl S, Kauhanen J, Toriola AT. Inflammatory biomarker score and cancer: a population-based prospective cohort study. *BMC Cancer*. 2016;16:80.
21. Imai Y, Ibata I, Ito D, Ohsawa K, Kohsaka S. A novel gene iba1 in the major histocompatibility complex class iii region encoding an EF hand protein expressed in a monocytic lineage. *Biochem Biophys Res Comm*. 1996;224:855–862.
22. Yurchenko E, Shio MT, Huang TC, Da Silva Martins M, Szyf M, Levings MK, Olivier M, Piccirillo CA. Inflammation-driven reprogramming of CD4+ Foxp3+ regulatory T cells into pathogenic Th1/Th17 t effectors is abrogated by mTOR inhibition in vivo. *PLoS One*. 2012;7:e35572.
23. Legroux L, Pittet CL, Beauseigle D, Deblois G, Prat A, Arbour N. An optimized method to process mouse CNS to simultaneously analyze neural cells and leukocytes by flow cytometry. *J Neurosci Methods*. 2015;247:23–31.
24. Massoud AH, Kaufman GN, Xue D, Beland M, Dembele M, Piccirillo CA, Mourad W, Mazer BD. Peripherally generated Foxp3(+) regulatory T cells mediate the immunomodulatory effects of IVIg in allergic airways disease. *J Immunol*. 2017;198:2760–2771.
25. Liesz A, Suri-Payer E, Veltkamp C, Doerr H, Sommer C, Rivest S, Giese T, Veltkamp R. Regulatory T cells are key cerebroprotective immunomodulators in acute experimental stroke. *Nat Med*. 2009;15:192–199.
26. Iulita MF, Vallerand D, Beauvillier M, Haupert N, C AU, Gagne A, Vernoux N, Duchemin S, Boily M, Tremblay ME, Girouard H. Differential effect of angiotensin II and blood pressure on hippocampal inflammation in mice. *J Neuroinflammation*. 2018;15:62.
27. Ghosh SK, Ekpo EB, Shah IU, Girling AJ, Jenkins C, Sinclair AJ. A double-blind, placebo-controlled parallel trial of vitamin c treatment in elderly patients with hypertension. *Gerontology*. 1994;40:268–272.
28. Schmidt A, Oberle N, Krammer PH. Molecular mechanisms of treg-mediated T cell suppression. *Front Immunol*. 2012;3:51.
29. Gonzalez P, Burgaya F, Acarin L, Peluffo H, Castellano B, Gonzalez B. Interleukin-10 and interleukin-10 receptor-I are upregulated in glial cells after an excitotoxic injury to the postnatal rat brain. *J Neuropathol Exp Neurol*. 2009;68:391–403.
30. Capone C, Faraco G, Park L, Cao X, Davisson RL, Iadecola C. The cerebrovascular dysfunction induced by slow pressor doses of angiotensin II precedes the development of hypertension. *Am J Physiol Heart Circ Physiol*. 2011;300:H397–H407.
31. Chrissobolis S, Banfi B, Sobey CG, Faraci FM. Role of Nox isoforms in angiotensin II-induced oxidative stress and endothelial dysfunction in brain. *J Appl Physiol*. 2012;113:184–191.
32. Paravicini TM, Touyz RM. NADPH oxidases, reactive oxygen species, and hypertension: clinical implications and therapeutic possibilities. *Diabetes Care*. 2008;31(suppl 2):S170–S180.
33. Serrano F, Kolluri NS, Wientjes FB, Card JP, Klann E. NADPH oxidase immunoreactivity in the mouse brain. *Brain Res*. 2003;988:193–198.
34. Cooney SJ, Bermudez-Sabogal SL, Byrnes KR. Cellular and temporal expression of NADPH oxidase (Nox) isotypes after brain injury. *J Neuroinflammation*. 2013;10:155.
35. Miller AA, Drummond GR, Sobey CG. Novel isoforms of nadph-oxidase in cerebral vascular control. *Pharmacol Ther*. 2006;111:928–948.
36. Faraco G, Sugiyama Y, Lane D, Garcia-Bonilla L, Chang H, Santisteban MM, Racchumi G, Murphy M, Van Rooijen N, Anrather J, Iadecola C. Perivascular macrophages mediate the neurovascular and cognitive dysfunction associated with hypertension. *J Clin Invest*. 2016;126:4674–4689.
37. Li P, Mao L, Zhou G, Leak RK, Sun BL, Chen J, Hu X. Adoptive regulatory T-cell therapy preserves systemic immune homeostasis after cerebral ischemia. *Stroke*. 2013;44:3509–3515.
38. Barcia C, Ros CM, Annese V, Gomez A, Ros-Bernal F, Aguado-Yera D, Martinez-Pagan ME, de Pablos V, Fernandez-Villalba E, Herrero MT. IFN-gamma signaling, with the synergistic contribution of TNF-alpha, mediates cell specific microglial and astroglial activation in experimental models of Parkinson's disease. *Cell Death Dis*. 2011;2:e142.
39. Reynolds AD, Stone DK, Mosley RL, Gendelman HE. Nitrated {alpha}-synuclein-induced alterations in microglial immunity are regulated by CD4+ T cell subsets. *J Immunol*. 2009;182:4137–4149.
40. Liu J, Gong N, Huang X, Reynolds AD, Mosley RL, Gendelman HE. Neuromodulatory activities of CD4+CD25+ regulatory T cells in a murine model of HIV-1-associated neurodegeneration. *J Immunol*. 2009;182:3855–3865.
41. Brea D, Agulla J, Rodriguez-Yanez M, Barral D, Ramos-Cabrer P, Campos F, Almeida A, Davalos A, Castillo J. Regulatory T cells modulate inflammation and reduce infarct volume in experimental brain ischaemia. *J Cell Mol Med*. 2014;18:1571–1579.
42. Cohen SL, Moore AM, Ward WE. Interleukin-10 knockout mouse: a model for studying bone metabolism during intestinal inflammation. *Inflamm Bowel Dis*. 2004;10:557–563.
43. Wei Z, Spizzo I, Diep H, Drummond GR, Widdop RE, Vinh A. Differential phenotypes of tissue-infiltrating T cells during angiotensin II-induced hypertension in mice. *PLoS One*. 2014;9:e114895.
44. Shi P, Diez-Freire C, Jun JY, Qi Y, Katovich MJ, Li Q, Sriramula S, Francis J, Sumners C, Raizada MK. Brain microglial cytokines in neurogenic hypertension. *Hypertension*. 2010;56:297–303.
45. Faraco G, Brea D, Garcia-Bonilla L, Wang G, Racchumi G, Chang H, Buendia I, Santisteban MM, Segarra SG, Koizumi K, Sugiyama Y, Murphy M, Voss H, Anrather J, Iadecola C. Dietary salt promotes neurovascular and cognitive dysfunction through a gut-initiated Th17 response. *Nat Neurosci*. 2018;21:240–249.
46. Nguyen H, Chiasson VL, Chatterjee P, Kopriva SE, Young KJ, Mitchell BM. Interleukin-17 causes rho-kinase-mediated endothelial dysfunction and hypertension. *Cardiovasc Res*. 2013;97:696–704.
47. Madhur MS, Lob HE, McCann LA, Iwakura Y, Blinder Y, Guzik TJ, Harrison DG. Interleukin 17 promotes angiotensin II-induced hypertension and vascular dysfunction. *Hypertension*. 2010;55:500–507.
48. Li P, Gan Y, Sun BL, Zhang F, Lu B, Gao Y, Liang W, Thomson AW, Chen J, Hu X. Adoptive regulatory T-cell therapy protects against cerebral ischemia. *Ann Neurol*. 2013;74:458–471.
49. Zhang M, Mao Y, Ramirez SH, Tuma RF, Chabrashvili T. Angiotensin II induced cerebral microvascular inflammation and increased blood-brain barrier permeability via oxidative stress. *Neuroscience*. 2010;171:852–858.
50. Meissner A, Minnerup J, Soria G, Planas AM. Structural and functional brain alterations in a murine model of angiotensin II-induced hypertension. *J Neurochem*. 2017;140:509–521.
51. Santisteban MM, Ahmari N, Carvajal JM, Zingler MB, Qi Y, Kim S, Joseph J, Garcia-Pereira F, Johnson RD, Shenoy V, Raizada MK, Zubcevic J. Involvement of bone marrow cells and neuroinflammation in hypertension. *Circ Res*. 2015;117:178–191.
52. Baruch K, Rosenzweig N, Kertser A, Deczkowska A, Sharif AM, Spinrad A, Tsitsou-Kampeli A, Sarel A, Cahalon L, Schwartz M. Breaking immune tolerance by targeting Foxp3(+) regulatory T cells mitigates Alzheimer's disease pathology. *Nat Commun*. 2015;6:7967.
53. Lokensgard JR, Schachtele SJ, Mutnal MB, Sheng WS, Prasad S, Hu S. Chronic reactive gliosis following regulatory T cell depletion during acute MCMV encephalitis. *Glia*. 2015;63:1982–1996.
54. Maes W, Verschuere T, Van Hoylandt A, Boon L, Van Gool S. Depletion of regulatory T cells in a mouse experimental glioma model through anti-CD25 treatment results in the infiltration of non-immunosuppressive myeloid cells in the brain. *Clin Dev Immunol*. 2013;2013:952469.
55. Mian MO, Barhoumi T, Briet M, Paradis P, Schiffrin EL. Deficiency of T-regulatory cells exaggerates angiotensin II-induced microvascular injury by enhancing immune responses. *J Hypertens*. 2016;34:97–108.

SUPPLEMENTAL MATERIAL

Data S1.

Supplemental Methods

Chronic angiotensin II and IL-10 infusion

Osmotic minipumps (model 1002, Alzet Durect Corp, USA) containing human Ang II (Millipore-Sigma, USA) were implanted subcutaneously under isoflurane anesthesia. Mice received bupivacaine hydrochloride (Marcaine, CDMV, Canada, 2 mg/kg s.c.) at the site of the incision before and after minipump implantation. Each osmotic pump delivered 1000 ng/kg/min for 14 days. Control animals received a sham surgery. Pilot experiments confirmed no differences between a sham surgery and implantation of a saline-infused minipump for cerebral blood flow analysis. In another group of animals, systemic infusion of 1000 ng of IL-10 was achieved via a second osmotic minipump filled with human recombinant IL-10 (Sigma-Aldrich, USA), delivering IL-10 at a rate of 60 ng/day. IL-10 minipumps were implanted together with the Ang II minipumps on the same day, for continued infusion during 14 days. There were no differential mortality events between the treated and control groups.

In vivo laser Doppler flowmetry

Anesthesia was initiated with isoflurane (induction: 5%, maintenance: 2%) and maintained by intraperitoneal injections of 50 mg/kg of alpha-chloralose (Santa Cruz Biotechnology, USA) and 750 mg/kg of urethane (Sigma-Aldrich, USA). Mean blood pressure and blood gases were monitored via femoral artery catheterization. Ventilation was maintained artificially with a nitrogen/oxygen/CO_2 mixture through a tracheal intubation. Body temperature was maintained at 37 ºC. Cerebral blood flow (CBF) was monitored by a laser Doppler probe (AD Instruments, USA) placed in a 2x2 mm cranial window drilled above the somatosensory cortex. Artificial cerebrospinal fluid (aCSF, NaCl 125 mM, KCl 3 mM, $NaHCO_3$ 26 mM, $NaH_2PO_4H_2O$ 1.25 mM, $CaCl_2$ 2 mM, $MgCl_26H_2O$ 1mM, glucose 4 mM, ascorbic acid 0.4 mM, bubbled with 95% O_2, 5% CO_2 for 10 minutes) was superfused (0.5 mL/min, 35 ºC) after the removal of the pia mater. Analysis of CBF responses began 30 minutes after the end of the surgery to allow blood gases to stabilize. Animals with a mean arterial blood pressure under 60 mmHg and/or blood gases outside normal range (pH: 7.35-7.40; pCO_2: 33-45; pO_2: 120-140) were eliminated from the study. This comprised 5 animals for the CBF experiments with wild-type $CD4^+CD25^+$ cells, 1 animal for the CBF experiment with the $CD4^+CD25^+$ *Il10*$^{-/-}$ cells and 6 animals for the CBF experiment with IL-10. The laser Doppler probe was placed stereotaxically above the whisker barrel area at the site of superfusion. CBF responses to neuronal activity were examined by whisker stimulation (three 1-minute stimulations at 6 Hz every 3 minutes on the contralateral side to CBF measurement). Endothelium-dependent CBF responses were measured after the superfusion of acetylcholine 10 μM (Sigma-Aldrich, USA), superfused for 5 minutes followed by a 15 minutes aCSF superfusion to restore basal stimulation level. CBF values were acquired with the LabChart6 Pro software (v6.1.3, AD Instruments, USA). The percentage increase in CBF was measured using the CBF values before the stimulations and the maximum response.

Blood pressure

Systolic blood pressure was monitored by non-invasive tail-cuff plethysmography (Kent Scientific Corp., USA). The measures were taken 24 hours before analysis of cerebral blood flow. Mice were warmed on a heating pad preheated at 37 °C for 10 minutes before and during blood pressure recordings. Animals were habituated to the procedure the three days prior to blood pressure assessment. On the experimental day, following stabilization, ten blood pressure measurements per mouse were done and averaged for analysis. Data were not considered valid if the blood flow in the tail was below 15 µL.

Plasma cytokine/chemokine array and composite score calculation

Blood was collected via cardiac puncture in heparinized tubes. Samples were centrifuged at 2000 g for 20 minutes at 4°C to separate plasma. Cleared plasma samples were stored at −80°C and were only thawed for cytokine/chemokine analysis. A multiplex bead-based immunoassay from Eve Technologies Corporation (Calgary, AB, Canada) was used for the quantitative determination of 31 mouse plasma cytokines and chemokines (MD31 Discovery Assay, Mouse Cytokine/Chemokine Array 31-Plex). Plasma samples were diluted in half in PBS pH 7.4 and shipped on dry ice for analysis. The array measured the levels of Eotaxin (CCL11), G-CSF, GM-CSF, IFNγ, IL-1α, IL-1β, IL-2, IL-3, IL-4, IL-5, IL-6, IL-7, IL-9, IL-10, IL-12 (p40), IL-12 (p70), IL-13, IL-15, IL-17A, IP-10 (CXCL10), KC (CXCL1), LIF, LIX (CXCL5), MCP-1 (CCL2), M-CSF, MIG (CXCL9), MIP-1α, MIP-1β (CCL4), MIP-2 (CXCL2), RANTES (CCL5), TNFα and VEGF. Analyte concentrations were expressed in pg/mL and calculated through a standard curve from fluorescence intensity values. The following were not included in the final analysis due to low or no detection in several samples: IL-3, IL-7, IFNγ, IL-1β, GM-CSF, M-CSF, VEGF and MIP-1α. Given the large number of cytokines/chemokines analyzed a composite inflammatory Z score was computed to obtain a global measure reflecting inflammation and providing a more powered analysis. Prior to composite score calculation and in consultation with an immunologist (Dr. Jean-François Gauchat, Université de Montréal, Canada), cytokines and chemokines were grouped into four categories according to their main function/immune effect: I) Pro-inflammatory cytokines: IL-1α, IL-6, IL-17, TNF-α and LIF; II) Neutrophil chemoattractants: KC (CXCL1), LIX (CXCL5), MIP-2 (CXCL2) and stimulators of their development (G-CSF); III) Stimulators of Th1-driven responses: IL-12p40, IL12p70, MIP-1β (CCL4), RANTES (CCL5), MIG (CXCL9) and IP-10 (CXCL10); IV) Stimulators of Th2-driven responses: IL-4, IL-5, IL-9, IL-10, IL-13 and MCP-1 (CCL2). Eotaxin (CCL11) and IL-2 were not classified in any of the groups and are presented independently. The grouping does not intend to reflect the cellular source of each cytokine but rather their main action/effect as immune mediators. Within each group a cytokine/chemokine composite score was calculated for each mouse by converting each independent marker to a standardized Z score, such that the group mean was zero and the standard deviation was 1. Z scores were obtained with the formula $z = (x - \mu) / \sigma$, where x was the individual value of the marker to be standardized, μ the mean of the dataset for that marker and σ the standard deviation. To generate the composite, Z scores within a group were added.

Microglia immunohistochemistry analysis

PFA-fixed brain sections (40 µm thick) were incubated in 0.3% hydrogen peroxide (Sigma-Aldrich, USA) for 20 minutes followed by 3 washes in PBS and 1 wash in PBS-T (PBS + 0.2% Triton X-100). Blocking was done with 10% normal goat serum in PBS-T during 1 hour at room temperature. Microglia/monocytes were labeled with Iba-1 (1:2000, Wako Inc, Richmond, USA) in PBS-T with 10% goat serum, overnight at 4 ºC. The following day, sections were washed in PBS-T and incubated in biotinylated goat anti-rabbit antibody (ABC Kit, Vector) at 1:500 in PBS-T with 5% goat serum for 1 h. Signal amplification was done following manufacturer's instructions. Immunoreactions were developed with 0.06% 3,3'-diaminobenzidine and 1% hydrogen peroxide (Sigma-Aldrich, USA) in PBS. Following mounting, sections were dehydrated and defatted in increasing ethanol concentrations and xylenes, then coverslipped. Bright field images were taken with a Leitz Diaplan microscope equipped with an Olympus DP21 camera (Wild Leitz GmbH, Germany). Images were taken from layer V-VI of the somatosensory cortex (8 pictures per brain section) and from the hippocampal regions CA1, CA3 and DG (2 pictures per region per brain section). Micrographs were imported into the ImageJ software for calculation of microglial cell number. Each 8-bit image was thresholded with the intermodes method and converted to binary. The 'Analyze Particles' function was used to obtain the approximate number of microglia in the whole micrograph, using a size criteria of 150 pixels. Three different brain sections per animal were examined, and an average per region was calculated per section. Each was used for analysis.

Superoxide anion production

Brain cortical superoxide anion production was measured by lucigenin-enhanced chemiluminescence using a scintillation counter (Wallac 1409, Perkin Elmer, Canada) in out-of-coincidence mode with a single active photomultiplier tube as previously described (Sadekova *et al*, JAHA 2013). Cortical tissue was incubated at 37°C for 15 minutes in an oxygenated Krebs-HEPES buffer in the presence of 100 µmol/L NADPH (Sigma-Aldrich, Canada). Following the addition of lucigenin (5 µmol/L, Sigma-Aldrich, Canada) counts were obtained at 1-minute intervals during 10 minutes and corrected for background (reaction done without brain tissue). Superoxide production was determined based on the area under the curve (AUC) of counts/time. A second cortical sample was first incubated with the selective NOX-2 inhibitor, gp91ds-tat (50 µmol/L, AnaSpec, USA), in Krebs-HEPES buffer during 45 minutes, followed by the addition of NADPH and lucigenin. Counts were obtained as described above. Given that lucigenin detects superoxide anions from various enzymatic oxidase systems, NOX-2-derived superoxide production was expressed as the percentage of inhibition by gp91ds-tat relative to the amount of superoxide produced without the inhibitor. Each value was normalized to tissue weight.

Table S1. Description of antibodies used for flow cytometry analysis.

Antigen	Fluorochrome	Clone	Manufacturer
CD3	BV737	17A2	BD Biosciences
CD11b	eFluor 450	M1/70	eBioscience ThermoFisher Scientific
F4/80	PeCy7	BM8	eBioscience ThermoFisher Scientific
CD11c	PercpCy5.5	HL3	BD Biosciences
CD19	APC	eBio1D3	eBioscience Thermofisher Scientific
Ly6G	Alexa700	1A8	Biolegend
CD45.2	APC-eFluor 780	104	eBioscience Thermofisher Scientific
CD49b	PE	DX5	eBioscience Thermofisher Scientific
Ki67	BUV395	B56	BD Biosciences
CD8a	PECy7	53-6.7	eBioscience Thermofisher Scientific
CD4	Alexa700	GK1.5	eBioscience Thermofisher Scientific
CD45.1	PercpCy5.5	A20	eBioscience Thermofisher Scientific
CD25	APC	PC61.6	eBioscience Thermofisher Scientific
CD3e	eFluor 450	17A2	eBioscience Thermofisher Scientific
Helios	PE	22F6	BD Biosciences

Table S2. Effect of $CD4^+CD25^+$ T lymphocytes on systolic blood pressure.

SBP (mmHg)	PBS	$CD4^+CD25^+$	$CD4^+CD25^+$ *Il10*$^{-/-}$
CTL	124.0 ± 2.5	129.3 ± 5.3	121.7 ± 9.9
Ang II	175.5 ± 6.0¶¶	177.4 ± 6.9¶	183.3 ± 6.3¶¶

Systolic blood pressure (SBP) was measured by tail-cuff plethysmography following 14 days of Ang II administration (1000 ng/kg/min) or a sham surgery for controls (CTL). Data is expressed as mean ± SEM, *n*=6-10/group; analyzed by two-way ANOVA, interaction: $F(2,37) = 0.539$ $p=0.589$; Ang II effect: $F(1,37) = 96.43$ $p<0.0001$; effect of $CD4^+CD25^+$ cells: $F(2,37) = 0.167$, $p=0.847$; ¶ $p<0.001$, ¶¶ $p<0.0001$ Ang II *versus* CTL

Table S3. Effect of exogenous IL-10 administration on systolic blood pressure.

SBP (mmHg)	PBS	IL-10
CTL	135.0 ± 1.7	132.8 ± 2.0
Ang II	172.3 ± 8.6¶	169.7 ± 2.3¶

Systolic blood pressure (SBP) was measured by tail-cuff plethysmography following 14 days of Ang II administration (1000 ng/kg/min) or Ang II + IL-10 (60 ng/day) or a sham surgery for controls (CTL). Data is expressed as mean ± SEM, n=3-6/group; analyzed by two-way ANOVA, interaction: $F(1,11) = 0.004$ p=0.952; Ang II effect: $F(1,11) = 83.63$ $p<0.0001$; effect of IL-10: $F(1,11) = 0.355$, p=0.563; ¶ $p<0.001$ Ang II *versus* CTL

Figure S1.

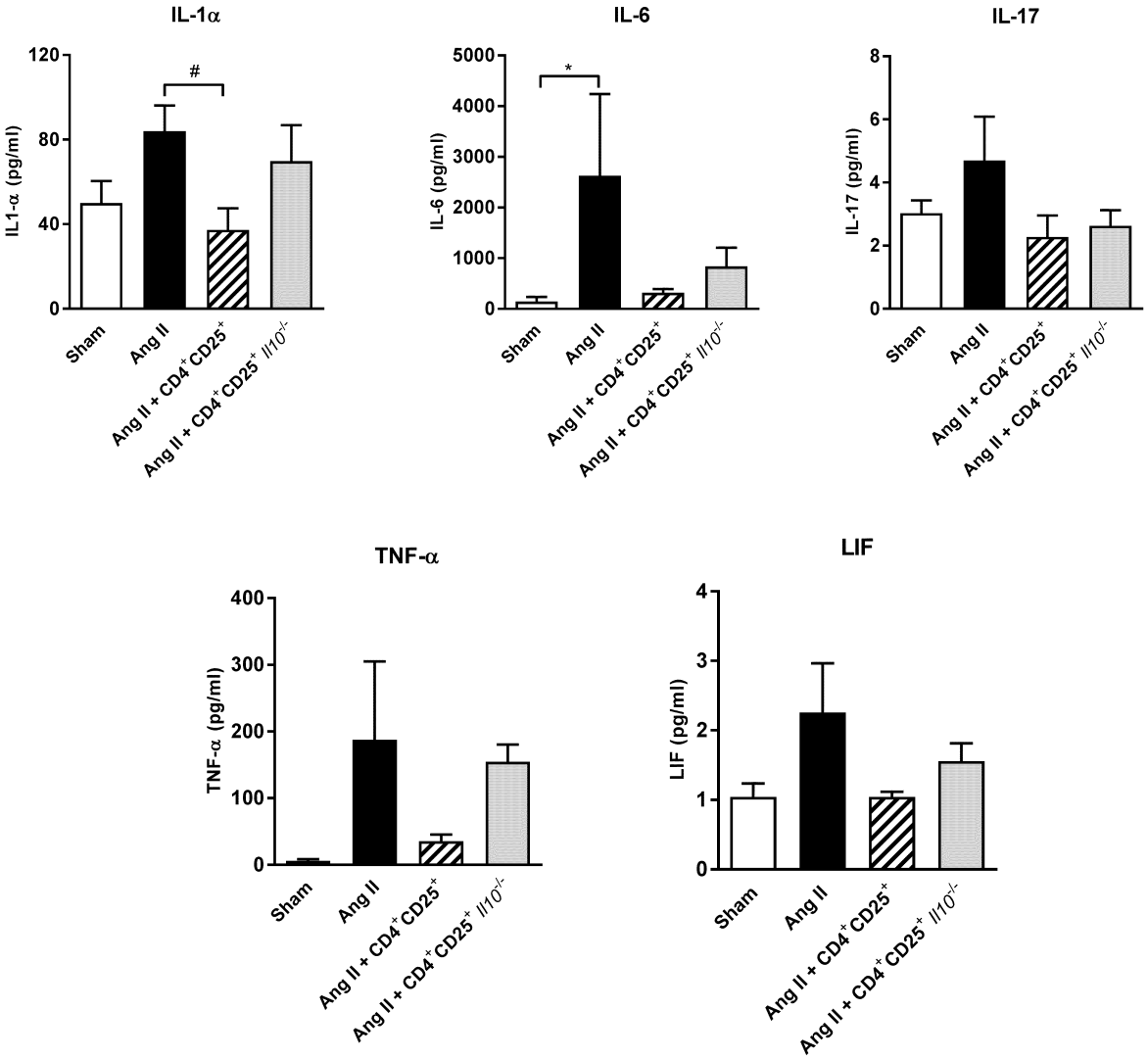

Figure S1. Effect of $CD4^+CD25^+$ adoptive transfer on plasma levels of pro-inflammatory cytokines induced by Ang II. The plasma levels (pg/ml) of individual pro-inflammatory cytokines were examined with a multiplex bead-based immunoassay following adoptive transfer of $CD4^+CD25^+$ or $CD4^+CD25^+$ *Il10*$^{-/-}$ cells or PBS in mice infused s.c. with Ang II (1000 ng/kg/min, 14 days) or in mice that received a sham surgery (Sham). Graphs represent mean ± SEM (n=4-11/group, *p<0.05 and #p<0.05 by one-way ANOVA followed by Bonferroni correction).

Figure S2.

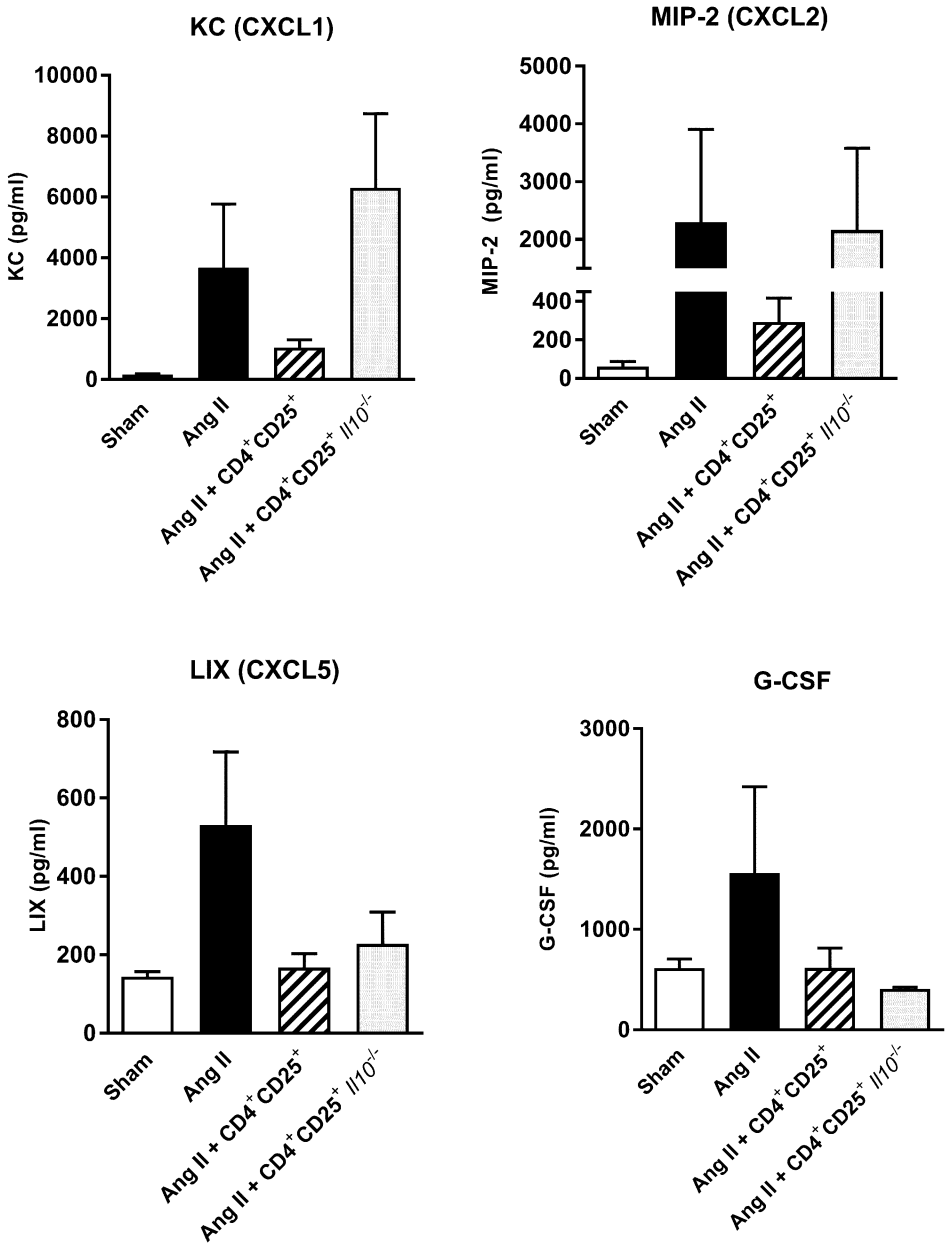

Figure S2. Effect of CD4$^+$CD25$^+$ adoptive transfer on plasma levels of neutrophil chemoattractants and stimulators of their development induced by Ang II. The plasma levels (pg/ml) of neutrophil chemoattractants (KC/CXCL1, MIP -2/CXCL2 and LIX/CXCL5) and stimulators of their development (G -CSF) were examined with a multiplex bead-based immunoassay following adoptive transfer of CD4 $^+$CD25$^+$ or CD4$^+$CD25$^+$ *Il10*$^{-/-}$ cells or PBS in mice infused s.c. with Ang II (1000 ng/kg/min, 14 days) or in mice that received a sham surgery (Sham). Graphs represent mean ± SEM (n=4-11/group, *p<0.05, by one-way ANOVA followed by Bonferroni correction).

Figure S3.

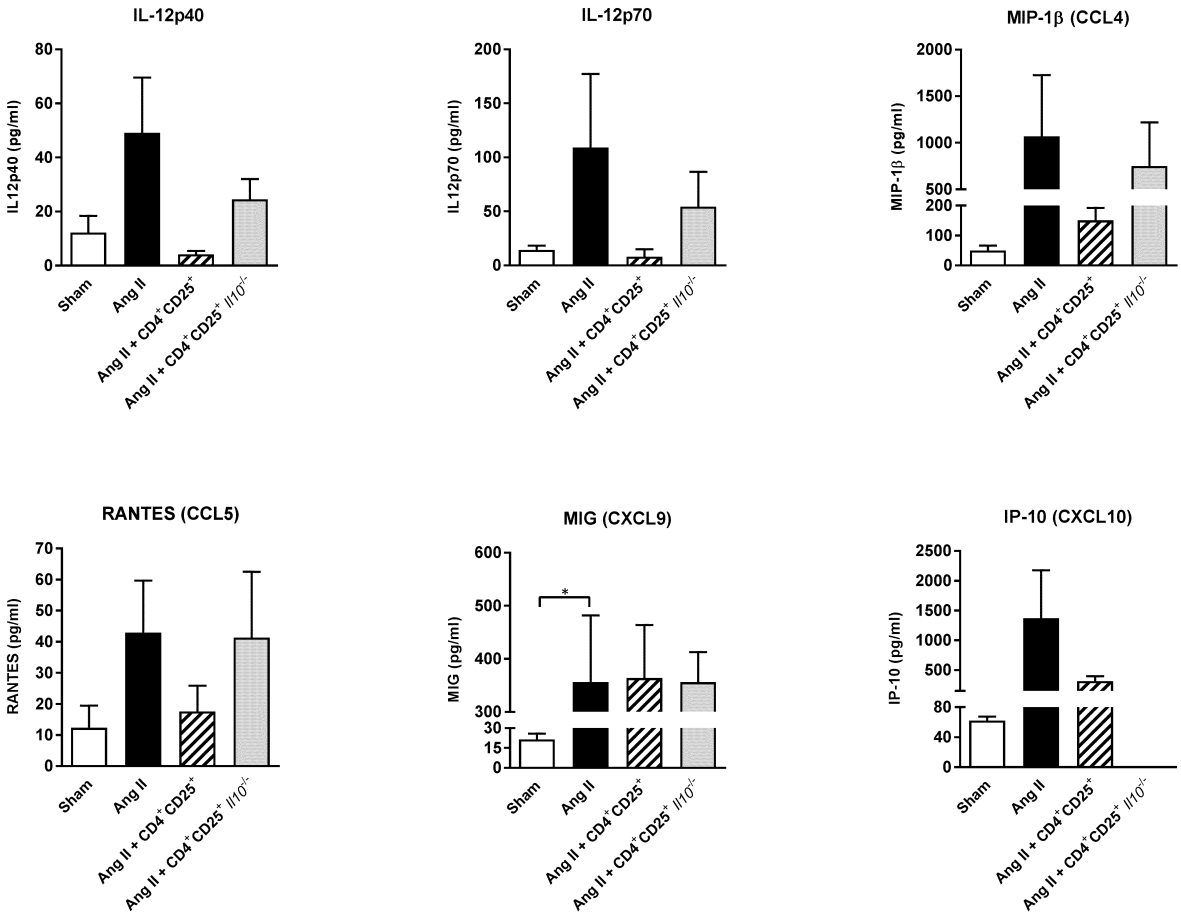

Figure S3. Effect of CD4$^+$CD25$^+$ adoptive transfer on plasma levels of stimulators of Th1-driven responses induced by Ang II. The plasma levels (pg/ml) of individual cytokines (IL-12p40 and IL-12p70) and chemokines (MIP-1β/CCL4, RANTES/CCL5, MIG/CCL9 and IP-10/CXCL10) involved in Th1 stimulation were examined with a multiplex bead-based immunoassay following adoptive transfer of CD4 $^+$CD25$^+$ or CD4$^+$CD25$^+$ *Il10*$^{-/-}$ cells or PBS in mice infused s.c. with Ang II (1000 ng/kg/min, 14 days) or in mice that received a sham surgery (Sham). Graphs represent mean ± SEM (n=4-11/group, * p<0.05, by one-way ANOVA followed by Bonferroni correction).

Figure S4.

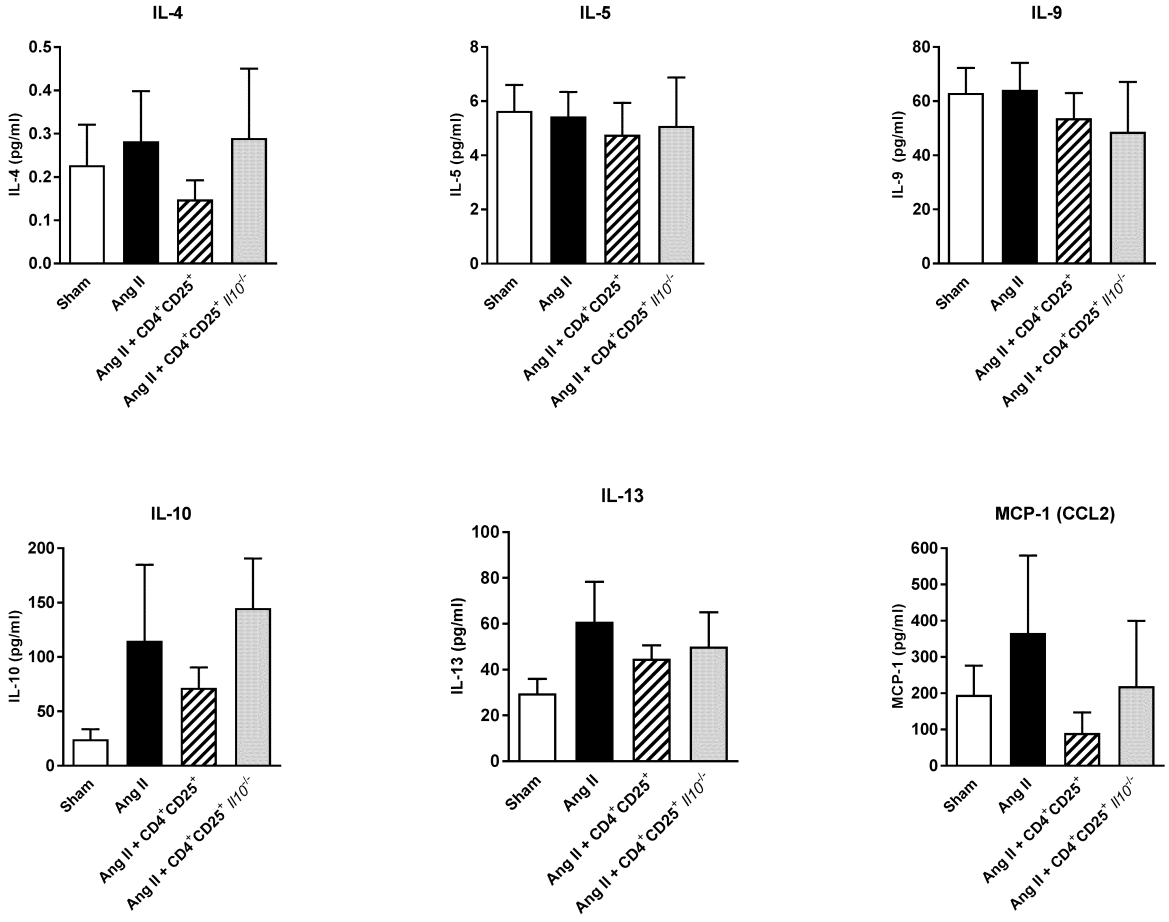

Figure S4. Effect of $CD4^+CD25^+$ adoptive transfer on plasma levels of stimulators of Th2-driven responses. The plasma levels (pg/ml) of cytokines (IL -4, IL-5, IL-9, IL-10 and IL-13) and chemokines (MCP -1/CCL2) involved in stimulation of Th2 responses were examined with a multiplex bead -based immunoassay following adoptive transfer of $CD4^+CD25^+$ or $CD4^+CD25^+$ *Il10*$^{-/-}$ cells or PBS in mice infused s.c. with Ang II (1000 ng/kg/min, 14 days) or in mice that received a sham surgery (Sham) . Graphs represent mean ± SEM (*n*=4-11/group, no significant differences between groups by one -way ANOVA followed by Bonferroni correction).

Figure S5.

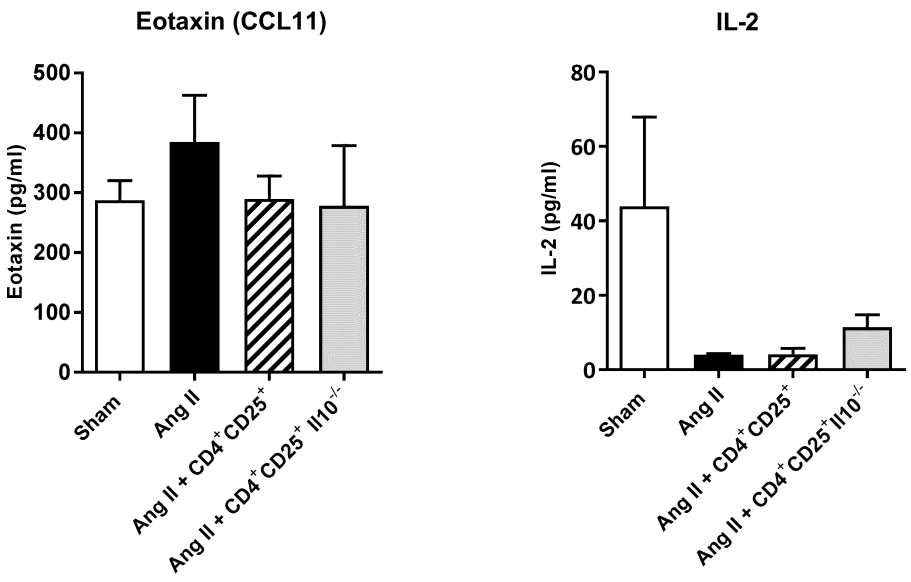

Figure S5. Effect of $CD4^+CD25^+$ adoptive transfer on plasma levels of eotaxin and IL-2 induced by Ang II. The plasma levels (pg/ml) of eotaxin (CCL11) and IL -2 were examined with a multiplex bead -based immunoassay following adoptive transfer of $CD4^+CD25^+$ or $CD4^+CD25^+$ *Il10*$^{-/-}$ cells or PBS in mice infused s.c. with Ang II (1000 ng/kg/min, 14 days) or in mice that received a sham surgery (Sham). Graphs represent mean ± SEM (*n*=4-11/group, no significant differences between groups by one -way ANOVA followed by Bonferroni correction).

Figure S6.

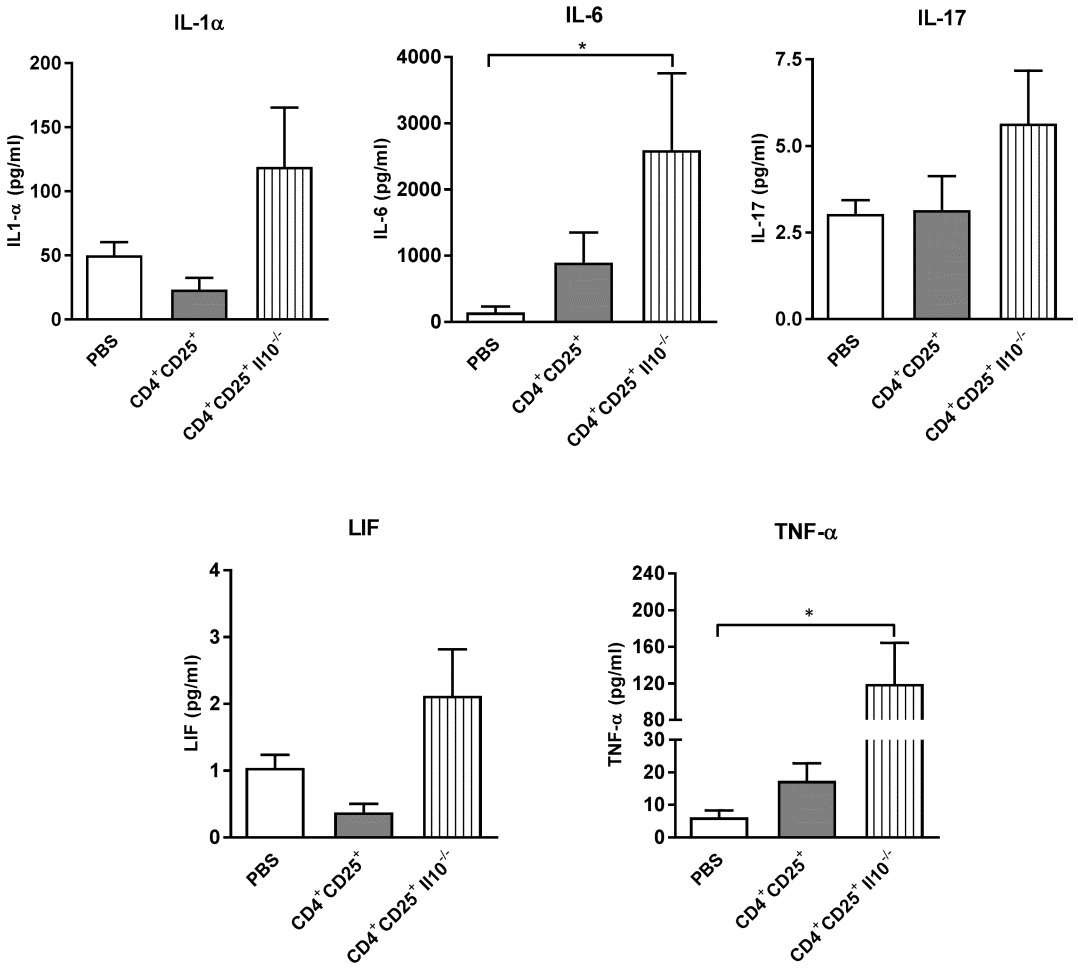

Figure S6. Effect of CD4$^+$CD25$^+$ *Il10*$^{-/-}$ adoptive transfer on plasma levels of pro -inflammatory cytokines in normal mice. The plasma levels (pg/ml) of pro -inflammatory cytokines were examined with a multiplex bead -based immunoassay following adoptive transfer of CD4$^+$CD25$^+$, CD4$^+$CD25$^+$ *Il10* $^{-/-}$ cells or PBS in C57BL/6 mice. Graphs represent mean ± SEM (n=4-11/group, *p<0.05, by one-way ANOVA followed by Bonferroni correction).

Figure S7.

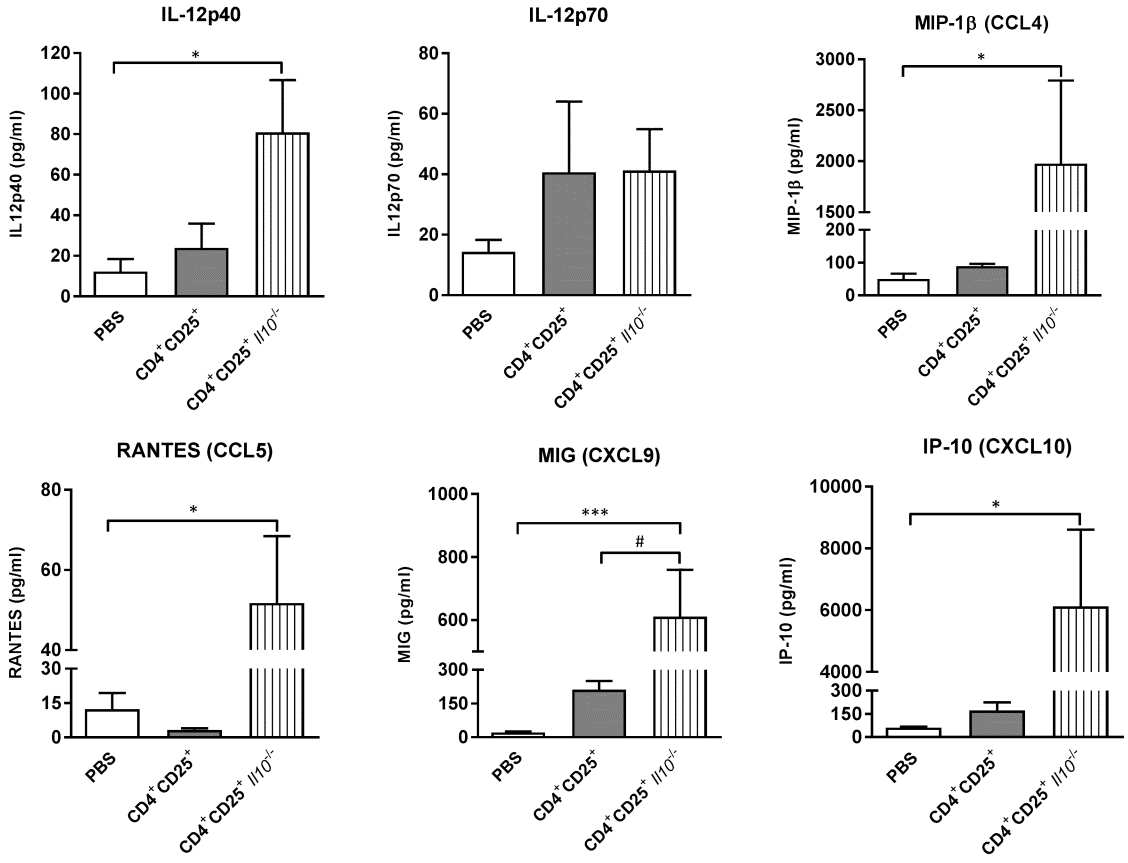

Figure S7. Effect of CD4^{+}CD25^{+} *Il10* $^{-/-}$ adoptive transfer on plasma levels of stimulators of Th1-driven responses in normal mice. The plasma levels (pg/ml) of cytokines (IL-12p40 and IL-12p70) and chemokines (MIP-1β/CCL4, RANTES/CCL5, MIG/CCL9 and IP-10/CXCL10) involved in Th1 stimulation were examined with a multiplex bead-based immunoassay following adoptive transfer of CD4 $^{+}$CD25^{+}, CD4^{+}CD25^{+} *Il10*$^{-/-}$ cells or PBS in C57BL/6 mice. Graphs represent mean ± SEM (n=4-11/group, *p<0.05, ***p<0.001, # p<0.05 by one-way ANOVA followed by Bonferroni correction).

Figure S8.

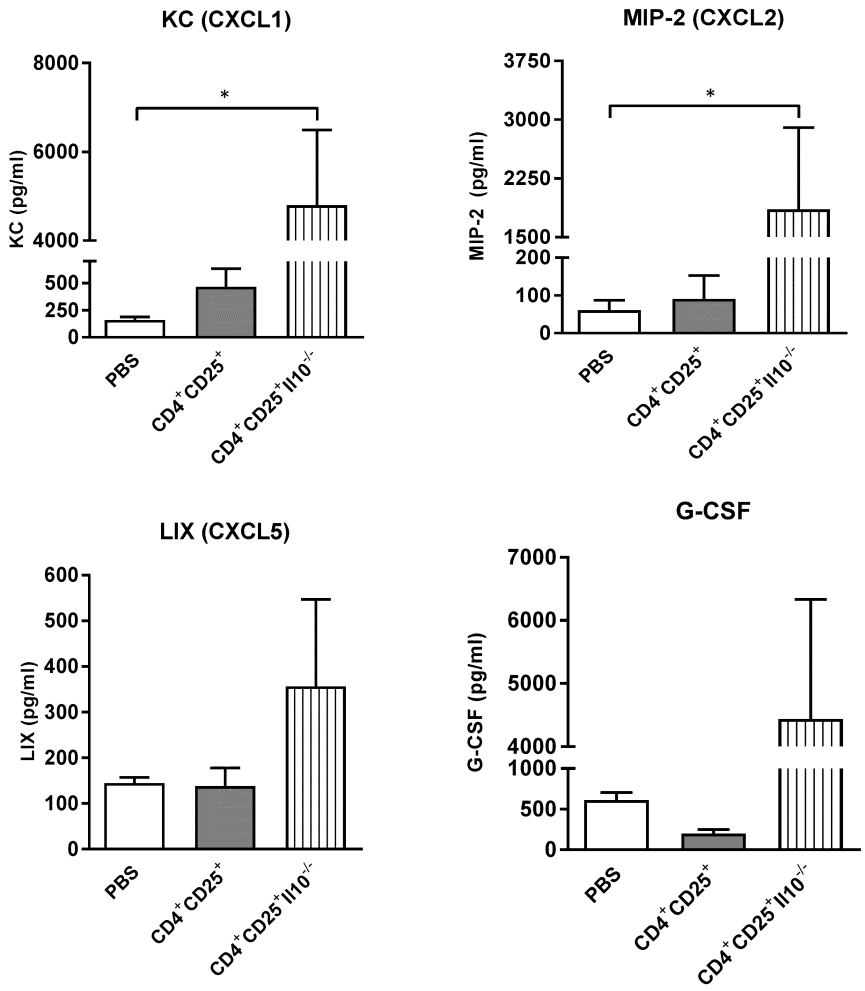

Figure S8. Effect of CD4$^+$CD25$^+$ *Il10* $^{-/-}$ adoptive transfer on plasma levels of neutrophil chemoattractants and stimulators of their development in normal mice. The plasma levels (pg/ml) of neutrophil chemoattractants (KC/CXCL1, MIP -2/CXCL2 and LIX/CXCL5) and stimulators of their development (G -CSF) were examined with a multiplex bead-based immunoassay following adoptive transfer of CD4 $^+$CD25$^+$, CD4$^+$CD25$^+$ *Il10*$^{-/-}$ cells or PBS in C57BL/6 mice. Graphs represent mean ± SEM (n=4-11/group, * p<0.05 by one-way ANOVA followed by Bonferroni correction).

Figure S9.

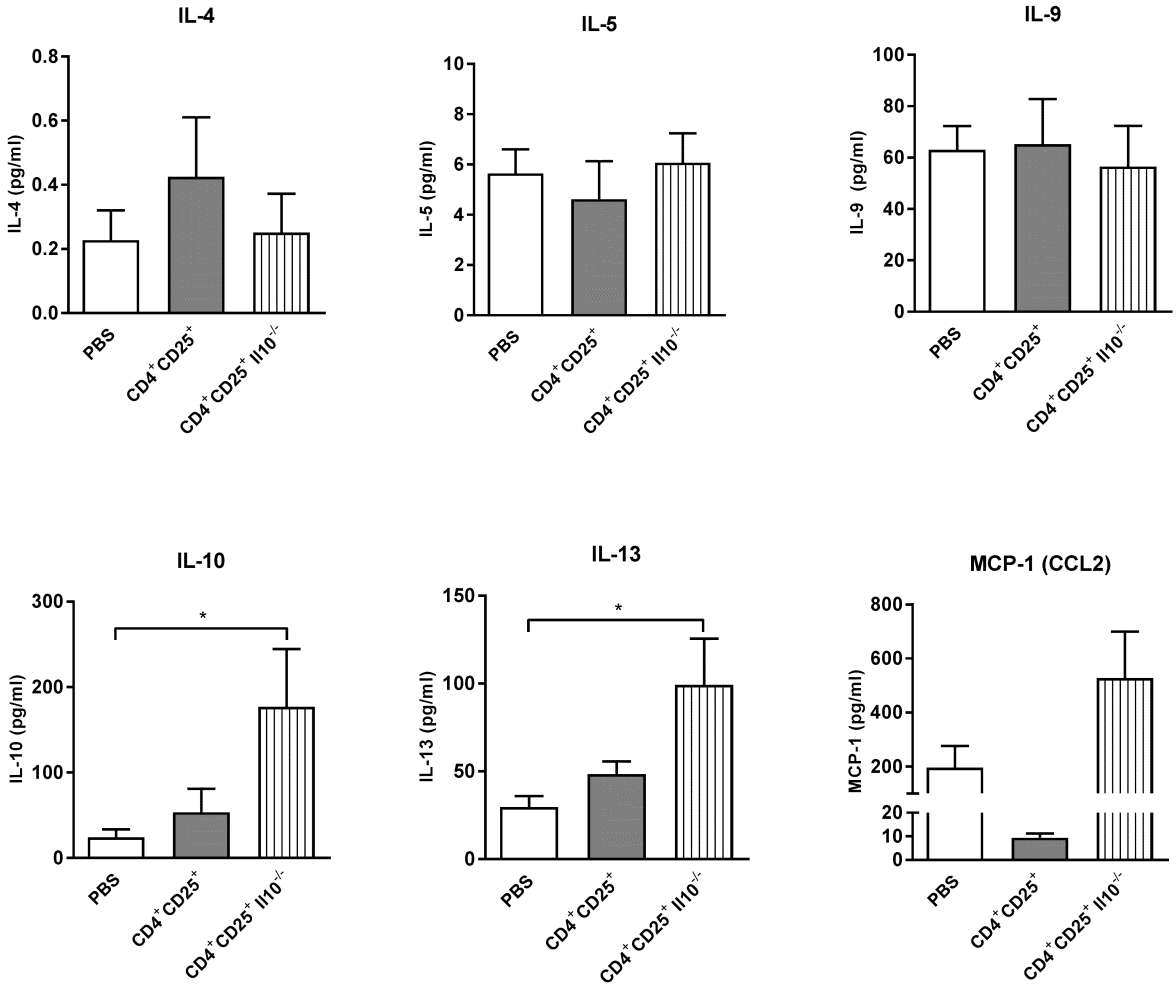

Figure S9. Effect of CD4^{+}CD25^{+} *Il10*$^{-/-}$ adoptive transfer on plasma levels of stimulators of Th2-driven responses in normal mice. The plasma levels (pg/ml) of cytokines (IL-4, IL-5, IL-9, IL-10 and IL-13) and chemokines (MCP-1/CCL2) involved in Th2 stimulation were examined with a multiplex bead-based immunoassay following adoptive transfer of CD4^{+}CD25^{+}, CD4^{+}CD25^{+} *Il10*$^{-/-}$ cells or PBS in C57BL/6 mice. Graphs represent mean ± SEM (n=4-11/group, *p<0.05, by one-way ANOVA followed by Bonferroni correction).

Figure S10.

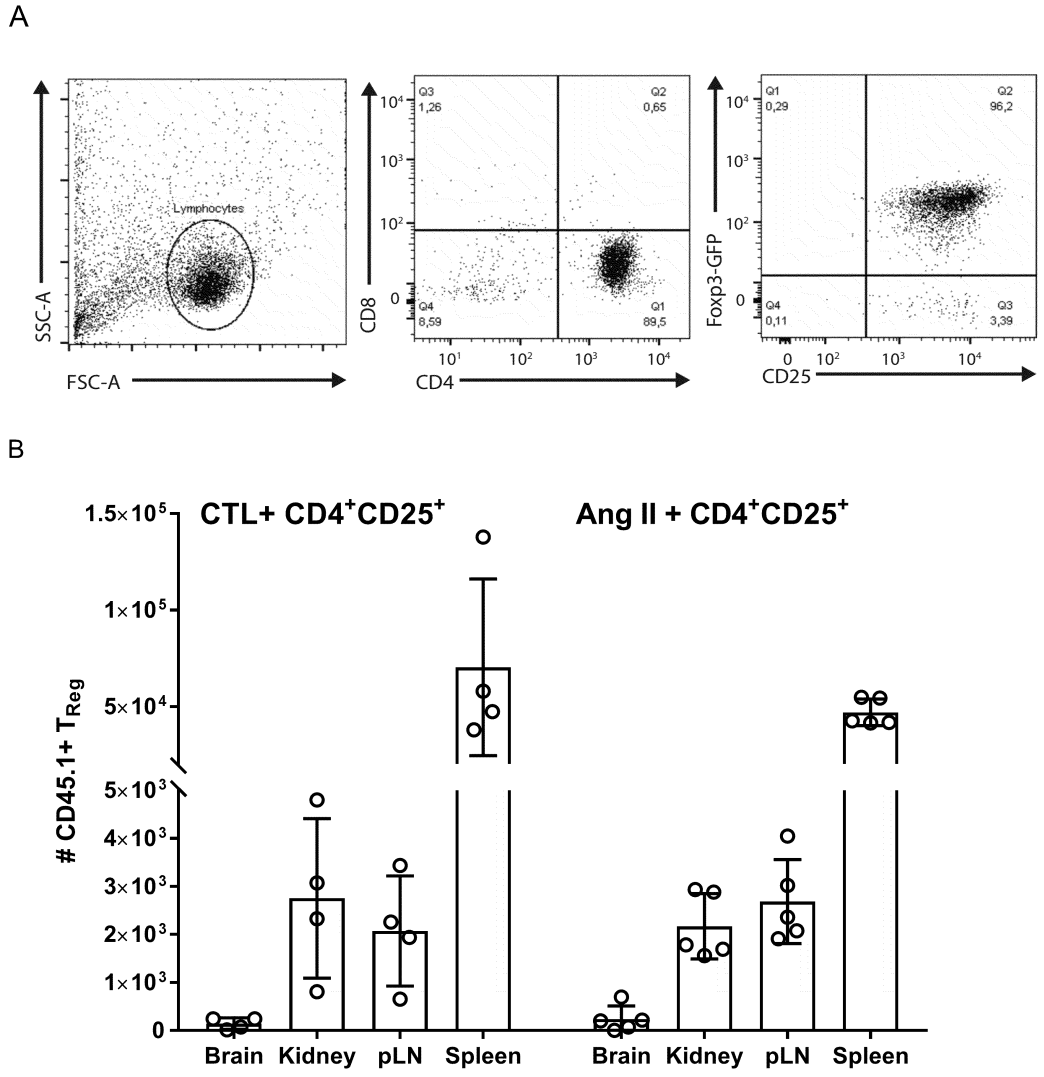

Figure S10. Analysis of Treg distribution. A) Flow cytometry analysis of the expression of CD8, CD4, Foxp3-GFP and CD25 from purified CD25 $^{+}$ cells isolated from the spleen of C57BL/6 Foxp3 ^{GFPki} CD45.1 $^{+}$ male mice by magnetic bead cell sorting (MACs® Miltenyi Biotec, Bergisch Gladbach, Germany) at the time of transfer (similar purity both at day 1 and day 7 of transfer); B) Analysis of cell suspensions of CD45.1 $^{+}$ exogenous Treg isolated from inguinal lymph nodes (pLN), spleen, and PBS-perfused brain and kidney dissected from C57BL/6 mice that received adoptive transfer of CD4 $^{+}$CD25 $^{+}$ cells (3x10 ^{5}) and were infused s.c. with Ang II (1000 ng/kg/min, 14 days) (Ang II + CD4 $^{+}$CD25 $^{+}$) or from mice that received a sham surgery (CTL+ CD4 $^{+}$CD25 $^{+}$).

Figure S11.

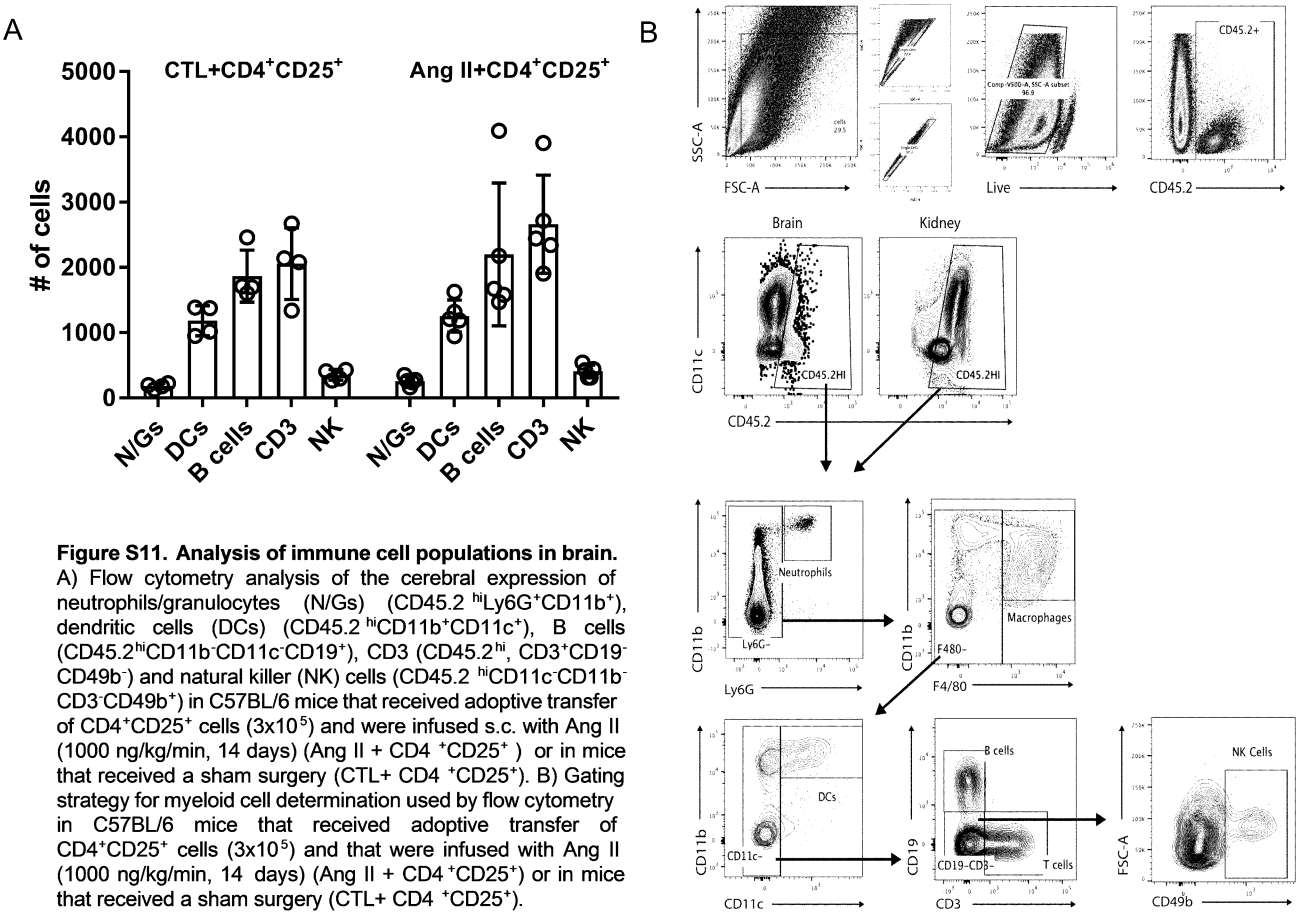

Figure S11. Analysis of immune cell populations in brain. A) Flow cytometry analysis of the cerebral expression of neutrophils/granulocytes (N/Gs) (CD45.2 ^{hi}Ly6G^{+}CD11b^{+}), dendritic cells (DCs) (CD45.2 ^{hi}CD11b^{+}CD11c^{+}), B cells (CD45.2^{hi}CD11b^{-}CD11c^{-}CD19^{+}), CD3 (CD45.2^{hi}, CD3^{+}CD19^{-} CD49b^{-}) and natural killer (NK) cells (CD45.2 ^{hi}CD11c^{-}CD11b^{-} CD3^{-}CD49b^{+}) in C57BL/6 mice that received adoptive transfer of CD4^{+}CD25^{+} cells (3x10^{5}) and were infused s.c. with Ang II (1000 ng/kg/min, 14 days) (Ang II + CD4 $^{+}$CD25^{+}) or in mice that received a sham surgery (CTL+ CD4 $^{+}$CD25^{+}). B) Gating strategy for myeloid cell determination used by flow cytometry in C57BL/6 mice that received adoptive transfer of CD4^{+}CD25^{+} cells (3x10^{5}) and that were infused with Ang II (1000 ng/kg/min, 14 days) (Ang II + CD4 $^{+}$CD25^{+}) or in mice that received a sham surgery (CTL+ CD4 $^{+}$CD25^{+}).